

MIT Open Access Articles

*Abyssal Upwelling and Downwelling
Driven by Near-Boundary Mixing*

The MIT Faculty has made this article openly available. **Please share** how this access benefits you. Your story matters.

Citation: McDougall, Trevor J., and Ferrari, Raffaele. "Abyssal Upwelling and Downwelling Driven by Near-Boundary Mixing." *Journal of Physical Oceanography* 47, 2 (February 2017): 261–283 © 2017 American Meteorological Society

As Published: <http://dx.doi.org/10.1175/jpo-d-16-0082.1>

Publisher: American Meteorological Society

Persistent URL: <http://hdl.handle.net/1721.1/111191>

Version: Final published version: final published article, as it appeared in a journal, conference proceedings, or other formally published context

Terms of Use: Article is made available in accordance with the publisher's policy and may be subject to US copyright law. Please refer to the publisher's site for terms of use.



Abyssal Upwelling and Downwelling Driven by Near-Boundary Mixing

TREVOR J. MCDUGALL

School of Mathematics and Statistics, University of New South Wales, Sydney, New South Wales, Australia

RAFFAELE FERRARI

Massachusetts Institute of Technology, Cambridge, Massachusetts

(Manuscript received 4 April 2016, in final form 31 October 2016)

ABSTRACT

A buoyancy and volume budget analysis of bottom-intensified mixing in the abyssal ocean reveals simple expressions for the strong upwelling in very thin continental boundary layers and the interior near-boundary downwelling in the stratified ocean interior. For a given amount of Antarctic Bottom Water that is upwelled through neutral density surfaces in the abyssal ocean (between 2000 and 5000 m), up to 5 times this volume flux is upwelled in narrow, turbulent, sloping bottom boundary layers, while up to 4 times the net upward volume transport of Bottom Water flows downward across isopycnals in the near-boundary stratified ocean interior. These ratios are a direct result of a buoyancy budget with respect to buoyancy surfaces, and these ratios are calculated from knowledge of the stratification in the abyss along with the assumed e -folding height that characterizes the decrease of the magnitude of the turbulent diapycnal buoyancy flux away from the seafloor. These strong diapycnal upward and downward volume transports are confined to a few hundred kilometers of the continental boundaries, with no appreciable diapycnal motion in the bulk of the interior ocean.

1. Introduction

The Antarctic Bottom Water (AABW) that sinks to the seafloor must rise through density surfaces in the abyss through the action of diapycnal mixing processes (together with a smaller role for geothermal heating). The classic “abyssal recipes” paper of Munk (1966) achieved this diapycnal upwelling via a one-dimensional advection–diffusion balance, which was consistent with a constant diapycnal diffusion coefficient of about $10^{-4} \text{ m}^2 \text{ s}^{-1}$ throughout the ocean interior. Since the buoyancy frequency increases with height, this one-dimensional advection–diffusion balance implies that the magnitude of the buoyancy flux and therefore the dissipation of turbulent kinetic energy is an increasing function of height; however, observations and theory over the past 20 yr have shown just the opposite, namely, that diapycnal mixing activity increases toward the seafloor.

In the past 20 yr, and particularly as a result of the Brazil Basin experiment of WOCE, observations and theory have shown that most of the diapycnal mixing

activity in the deep ocean occurs above rough bottom topography and is bottom intensified with an e -folding height above the bottom with a typical vertical e -folding length scale of $\sim 500 \text{ m}$ (Kunze et al. 2006).

The decrease of the magnitude of the diapycnal buoyancy flux with height above the bottom causes a downwelling diapycnal velocity, and this raises the question of how AABW can upwell across isopycnals when the diapycnal mixing activity profile on every vertical cast implies downwelling. Polzin et al. (1997) and St. Laurent et al. (2001) were aware of this apparent conundrum in the interior of the Brazil Basin, and they realized that the zero-flux condition at the seafloor meant that there must be diapycnal upwelling in the bottom boundary layer. Klocker and McDougall (2010) emphasized that the overall buoyancy budget can be satisfied while having the mean diapycnal motion being upward if the area of isopycnals increase with height; that is, the conundrum of how water can be upwelled diapycnally while having the magnitude of the diapycnal buoyancy flux increase toward the seafloor on every vertical cast cannot be resolved in an ocean with vertical sidewalls but is possible with a sloping seafloor. However, their area-integrated buoyancy argument did not resolve the question of exactly where and how the water

Corresponding author e-mail: Trevor J. McDougall, trevor.mcdougall@unsw.edu.au

upwells through isopycnals, although with hindsight, and through the process of elimination, it is clear that this diapycnal upwelling must occur very near the sloping boundary, as predicted by [St. Laurent et al. \(2001\)](#).

[De Lavergne et al. \(2016\)](#) have diagnosed the negative diapycnal transport in the ocean interior caused by near-boundary breaking internal waves, and they have pointed toward the important role of the turbulent bottom boundary layer (BBL) in order to upwell the AABW and to close the circulation. [Ferrari et al. \(2016\)](#) have studied the crucial role of these BBLs in allowing sufficiently strong upwelling across isopycnals therein to overcome the downwelling in the near-boundary stratified interior, while farther away from the ocean boundaries there is almost no diapycnal motion. This view of the abyssal circulation contrasts sharply with our previous view of the diapycnal upwelling being distributed uniformly over the deep-ocean basins. [Ferrari et al. \(2016\)](#) showed that both in idealized numerical simulations and in the real ocean, the upwelling in the narrow turbulent boundary layers varied from 2 to 3 times the mean upwelling transport of AABW.

The feature that causes this rather dramatic change in where we expect diapycnal motion in the abyss is the bottom intensification of the diapycnal buoyancy flux. In the present paper, we examine the volume-integrated buoyancy budget between pairs of buoyancy surfaces in the abyss using the Walin framework for including the influence of diapycnal transports and the boundary flux of buoyancy (i.e., the geothermal heat flux). The buoyancy budget for the whole ocean volume beneath a certain buoyancy surface is given by the very simple Eq. (12), which shows that in steady state the magnitude of the diffusive flux of buoyancy across this buoyancy surface is equal to the integral with respect to buoyancy of the net diapycnal upwelling below this buoyancy surface. By assuming that the bottom intensification occurs in an exponential fashion with height, we are able to relate the downward diapycnal volume transport in the near-boundary ocean interior [called the stratified mixing layer (SML)] to the total diapycnal diffusive buoyancy flux across a buoyancy surface. This leads to very simple expressions [Eqs. (13) and (14)] for both the upwelling diapycnal volume flux in the BBL and the downwelling diapycnal volume flux in the SML in terms of the net upwelling of AABW in the abyss. The application of the Walin budget framework with respect to density surfaces in the abyss, and the resulting Eqs. (13) and (14) are the main results of this paper.

One of the main conclusions is that the magnitude of the area-integrated buoyancy flux F on a global buoyancy surface must be an increasing function of buoyancy in order to have net upwelling through a stably stratified

ocean. As pointed out by [Klocker and McDougall \(2010\)](#), this upwelling needs to be achieved despite the fact that the magnitude of the turbulent buoyancy flux is a decreasing function of height on each vertical profile. Nonetheless, the ocean has found a way to achieve the net upwelling of bottom waters, and the secret lies in the BBLs ([St. Laurent et al. 2001](#); [de Lavergne et al. 2016](#); [Ferrari et al. 2016](#)).

There are two ways of ensuring that the magnitude of the area-integrated buoyancy flux increases with buoyancy (height). First, the magnitude of the buoyancy flux just above the turbulent boundary layer B_0 can be an increasing function of buoyancy, and second, the area of the SML can increase with buoyancy. Neither of these ways of achieving the increase with buoyancy of the magnitude of the area-integrated buoyancy flux (i.e., $dF/db > 0$) were considered in the seminal boundary mixing descriptions of [Thorpe \(1987\)](#), [Garrett \(1990, 1991, 2001\)](#), or [Garrett et al. \(1993\)](#) except perhaps in their reference to the “tertiary circulation” of [Phillips et al. \(1986\)](#) and [McDougall \(1989\)](#).

Our focus is on the mixing in the stratified ocean interior, and this focus is crucial. This region of mixing was also the focus of [Klocker and McDougall \(2010\)](#), [de Lavergne et al. \(2016\)](#), and [Ferrari et al. \(2016\)](#). Mixing very close to the sloping seafloor suffers from two effects that make the mixing processes there particularly ineffective at contributing to the flux of buoyancy. First, the mixing efficiency is reduced in this boundary region because the stratification is observed to become very small, and second, there is a “secondary circulation” that was found by [Garrett \(1990, 2001\)](#) to dramatically reduce the net vertical flux of buoyancy. [Armi \(1979\)](#) and [Garrett \(1990\)](#) both made the point that if near-boundary mixing were to make a significant contribution, then it would need to occur in the stratified near-boundary region. This is exactly the SML region in which the enhanced diapycnal mixing above rough topography is observed to occur.

The classic boundary mixing papers of [Wunsch \(1970\)](#), [Phillips \(1970\)](#), [Thorpe \(1987\)](#), and many of the Garrett papers solve both the momentum and buoyancy equations, but in this paper we ignore the momentum balance and concentrate only on the buoyancy equation, as did [Garrett \(2001\)](#). Furthermore, along an isopycnal near a sloping boundary the interior ocean is divided into two regions depending on the sign of the diapycnal velocity.

In this paper, we concentrate on the diapycnal upwelling and downwelling in the abyssal ocean for density classes that outcrop in the Southern Ocean but do not outcrop in the North Atlantic, so that it is clear that the upwelling must occur diapycnally in the ocean interior

(Talley 2013). Throughout this paper we use the term upwelling to mean the diapycnal upwelling through buoyancy surfaces (rather than through geopotential surfaces as is sometimes meant by the word upwelling). By performing our analysis with respect to density surfaces, the strong isopycnal flows and isopycnal turbulent stirring and mixing do not enter our equations. That is, while these strong epineutral mixing processes will be effective at diluting any tracer signature of near-boundary diapycnal mixing processes into the ocean interior, they do not enter or complicate our analysis of diapycnal mixing and advection in density coordinates.

2. Diapycnal volume transports expressed in terms of the turbulent buoyancy fluxes and the geothermal heat flux

In the present work, we represent the boundary region in a particularly simple manner. We allow a turbulent boundary layer right against the sloping seafloor in which the isopycnals are assumed to be normal to the seafloor, and at the top of this turbulent boundary layer we have assumed that the stratification abruptly changes to have the isopycnals essentially flat.

The vertical profile of the magnitude of the diapycnal buoyancy flux \mathcal{B} in the deep ocean is taken to be zero at the seafloor and to increase with height in the BBL to a maximum value of \mathcal{B}_0 at the top of the BBL of thickness h and then to decrease exponentially with height (with scale height d) in the SML (see Fig. 1). The influence of the geothermal heat flux at the seafloor is secondary, as discussed below. The turbulent buoyancy flux can be written in terms of the turbulent diffusivity D acting on the vertical gradient of buoyancy b_z as the downgradient flux $-Db_z$ (and note that $b_z = N^2$). We choose to frame the discussion in terms of the magnitude of the turbulent buoyancy flux per unit area, which we give the symbol \mathcal{B} so that in the ocean interior we have $\mathcal{B} = Db_z$. Measurements of the dissipation of turbulent kinetic energy per unit mass ε are often used to estimate \mathcal{B} as $\mathcal{B} = \Gamma\varepsilon$, where Γ is the mixing efficiency following Osborn (1980). In the BBL it is the strong variation of the mixing efficiency Γ with height that is responsible for the magnitude of the buoyancy flux per unit area going from \mathcal{B}_0 at the top of the boundary layer to zero at the seafloor (in the absence of the geothermal heat flux).

We examine the buoyancy budget for the volume between two closely spaced buoyancy surfaces b and $b + \Delta b$, bounded by a sloping seafloor, as shown in Fig. 2, following the approach of the appendix of Klocker and McDougall (2010) and the volume-integrated buoyancy and volume conservation approach of Walin (1982). We ignore several subtleties of the equation of state of

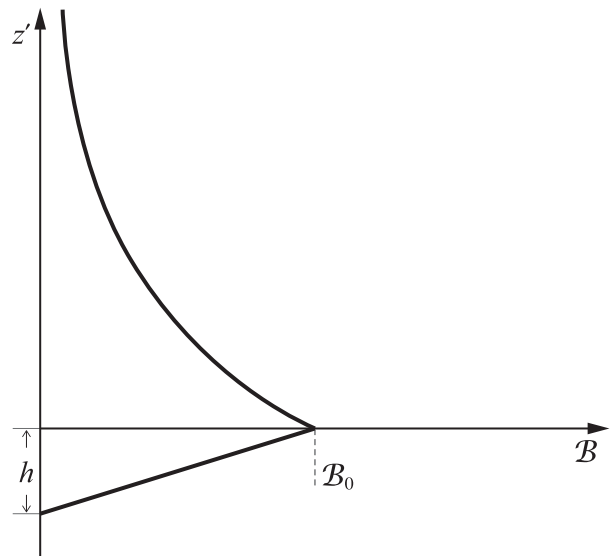


FIG. 1. In the deep ocean each vertical cast is assumed to have the magnitude of the diffusive buoyancy flux \mathcal{B} start at zero at the seafloor and to increase with height in the turbulent BBL to a maximum value of \mathcal{B}_0 at the top of the BBL of thickness h and then decrease exponentially toward zero as $\mathcal{B}_0 \exp(-z'/d)$, where z' is the height above the top of the turbulent boundary layer.

seawater and we take the vertical gradient of buoyancy b_z to be equal to the square of the buoyancy frequency, that is, $N^2 = b_z$, and we use subscripts to denote differentiation. Because the mixing intensity decreases smoothly in the vertical, the shaded control volume of Fig. 2b actually extends all the way to the right in the figure even though the shading is shown ending where the mixing intensity becomes sufficiently small. Along the upper $b + \Delta b$ surface the magnitude of the diffusive buoyancy flux is the maximum value \mathcal{B}_0 on that buoyancy surface at point a and decreases to the right, that is, away from the boundary along the buoyancy surface. Similarly, along the lower buoyancy surface, the magnitude of the diffusive buoyancy flux is the maximum value \mathcal{B}_0 on that buoyancy surface at point b and decreases to the right (the values of \mathcal{B}_0 at points a and b may be different).

The seawater nearest the sloping seafloor is assumed to be well mixed in a turbulent fashion, and the zero-flux boundary condition (in the absence of the geothermal heat flux) implies that the isolines of buoyancy are normal to the seafloor at this boundary. The bottom mixed layer properties such as the flow speed in the boundary layer are taken to be independent of height in the boundary layer, implying that the divergence of the turbulent flux of buoyancy is also independent of height inside the boundary layer. This is the motivation for why we have taken the magnitude of the buoyancy flux \mathcal{B} to

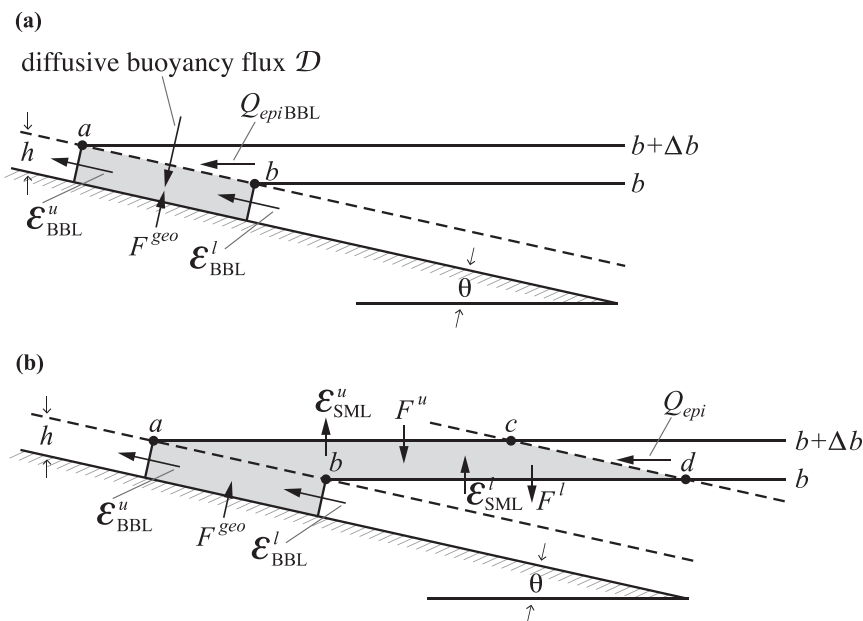


FIG. 2. The geometry of the near-boundary mixing region, concentrating on the volume between two closely spaced buoyancy surfaces. The turbulent BBL against the solid boundary has thickness h . The area integral of the diffusive flux of buoyancy, whose magnitude is F , is directed downward while the diapycnal velocity e and the diapycnal volume fluxes \mathcal{E}_{SML} and \mathcal{E}_{BBL} are defined positive upward. (a) The fluxes required to establish the buoyancy budget for the turbulent BBL; (b) the corresponding terms needed for the buoyancy budget for the whole shaded near-boundary region that includes the BBL.

vary linearly with height in the boundary layer from the value B_0 at the top of the turbulent boundary layer to zero at the bottom.

The area of active mixing to the right of point a of the upper isopycnal in Fig. 2b is not necessarily taken to be equal to that to the right of point b of the lower isopycnal because, for example, the sloping wall may well be part of a surface of revolution, so that if this slope $\tan\theta$ is the continental boundary of a circular ocean, then the area of active mixing on the upper isopycnal will be larger than that on the lower surface. Conversely, if the slope is the sloping boundary of a seamount with a depth-independent slope, the area of active mixing on the lower (annular) surface will exceed that of the upper surface.

The horizontal distance of active mixing on the upper isopycnal scales as $d/\tan\theta$, which for small slopes far exceeds the corresponding distance $h\cos\theta$ along this isopycnal inside the well-mixed turbulent boundary layer of depth h . Because of this, and also because $|\nabla b|$ is smaller in the boundary layer by a factor of $\sin\theta$, compared with the gradient in the stratified ocean interior b_z , when evaluating the total diffusive flux of buoyancy across the upper isopycnal, we may ignore the contribution from the area that lies inside the turbulent boundary layer and consider only the contribution from the area to the right of point a of Fig. 2. The same applies to the lower density surface.

We define the magnitude of the diffusive buoyancy flux across the whole interior area of an isopycnal as

$$F = \iint \mathcal{B}(b, x, y) dx dy, \quad (1)$$

where it is recognized that this integral only needs to be performed along the near-boundary SML where the dissipation is significantly nonzero. That is, because \mathcal{B} decreases rapidly with height, it also decreases very strongly with horizontal distance from the sloping boundary (to the right) in Fig. 2b. The integral in Eq. (1) is performed on a buoyancy surface so that F is a function only of buoyancy b .

The volume and buoyancy budgets of the shaded fluid of Figs. 2a and 2b are examined in appendix A, where the following results are found for the diapycnal volume transports in the turbulent BBL \mathcal{E}_{BBL} and net diapycnal volume transport \mathcal{E}_{net} , being the sum of \mathcal{E}_{BBL} and the diapycnal volume transport across the buoyancy surface in the SML \mathcal{E}_{SML} :

$$\mathcal{E}_{BBL} = \int \frac{G + \mathcal{B}_0}{b_z} \frac{1}{\tan\theta} dc, \quad \text{and} \quad (2)$$

$$\mathcal{E}_{net} \equiv \mathcal{E}_{BBL} + \mathcal{E}_{SML} = \frac{dF}{db} + \int \frac{G}{b_z} \frac{1}{\tan\theta} dc. \quad (3)$$

The difference between these two equations gives the following expression for \mathcal{E}_{SML} :

$$\mathcal{E}_{\text{SML}} = \frac{dF}{db} - \int \frac{\mathcal{B}_0}{b_z} \frac{1}{\tan\theta} dc. \quad (4)$$

These statements for the various diapycnal volume transports apply locally to an area of diapycnal mixing near a boundary, and they apply even when the flow is not in a steady state and also when the near-boundary layer region receives (or exports) volume from/to the rest of the ocean. That is, a complete integration over the full area of a buoyancy surface is not needed to obtain these results; these three equations are applicable to a local area of mixing and also to the integral over a complete isopycnal, and they apply whether the ocean is stationary or nonstationary. The key assumptions we have made are that (i) the amplitude of turbulent diapycnal mixing decreases toward zero as one moves sufficiently far from the sloping boundary and (ii) that a well-mixed turbulent boundary layer exists very close to the sloping solid boundary. At this stage we have not assumed the functional form for the decrease of mixing intensity with height.

In these equations dF/db is the rate at which the magnitude of the isopycnally area-integrated turbulent buoyancy flux F varies with respect to the buoyancy label b of the isopycnals; G and \mathcal{B}_0 are the fluxes of buoyancy into the turbulent BBL per unit of exactly horizontal area due to the geothermal heat flux G and the diffusive buoyancy flux at the top of the BBL \mathcal{B}_0 , respectively; θ is the angle that the bottom topography makes with the horizontal; and dc is the element of spatial integration into the page of Fig. 2.

Equation (2) shows that the sum of the geothermal heat flux per unit area at the seafloor G and the magnitude of the turbulent buoyancy flux per unit area at the top of the BBL \mathcal{B}_0 drive a net upwelling volume transport along the BBL. The diapycnal upwelling transport \mathcal{E}_{BBL} increases as the seafloor slope $\tan\theta$ decreases, and it increases in proportion to the circumference (or perimeter) of the edge of the isopycnal where it intersects the ocean boundary. Equation (3) confirms that the net diapycnal upwelling is proportional to the increase with buoyancy of the magnitude of the area-integrated turbulent buoyancy flux, as discussed in the introduction, plus the geothermal contribution coming into the BBL. Coming to grips with Eq. (4) for the diapycnal sinking in the SML and its relationship to the BBL and net transports is a main focus of this work.

Klocker and McDougall (2010) applied this buoyancy budget approach to the whole area of a neutral density surface in the interior of the deep ocean, and they wrote

the volume-integrated buoyancy budget corresponding to our Eq. (3) as $AeN^2 = (A\Gamma\varepsilon)_z$ [see their Eq. (26), once the effects of the nonlinear nature of the equation of state are ignored in that equation and noting that their derivation did not include the geothermal heat flux], where the product Ae stood for the area integral of the dianeutral velocity (i.e., \mathcal{E}_{net}) and $A\Gamma\varepsilon$ stood for the area integral of the magnitude of the diffusive buoyancy flux, which we now label F . Ferrari et al. (2016) wrote this volume-integrated buoyancy budget as their Eqs. (6) to (8), and they distinguished between the dianeutral advection that occurs in the ocean interior \mathcal{E}_{SML} versus that occurring in the boundary layer \mathcal{E}_{BBL} . In this work, we continue to make this important distinction and to estimate the relative magnitudes of these two dianeutral volume fluxes.

3. Diapycnal volume transports driven by the geothermal heat flux and the background turbulent diffusivity

It is apparent from the above equations that the geothermal buoyancy flux contributes to the diapycnal volume flux in the BBL but does not contribute to the near-boundary diapycnal volume flux in the SML \mathcal{E}_{SML} . In most of this paper it is convenient to ignore the influence of the geothermal heat flux from the discussion, but before doing so we will first estimate its magnitude. In a ground-breaking study of the effect of the geothermal heat flux on the abyssal circulation, Emile-Geay and Madec (2009) showed that the geothermal heat flux supplied heat to the BBL equivalent to what would be provided by a diapycnal diffusivity of potential temperature of approximately $1.2 \times 10^{-4} \text{ m}^2 \text{ s}^{-1}$ immediately above the BBL. Bearing in mind that the stability ratio $R_\rho = (\alpha\Theta_z)/(\beta S_{A_z})$ is approximately 2 in the abyssal ocean, this observation of Emile-Geay and Madec (2009) means that we may approximate G/b_z in Eq. (2) by a vertical diffusivity of buoyancy of approximately $2 \times 10^{-4} \text{ m}^2 \text{ s}^{-1}$. Taking the perimeter of the global ocean at a depth of 2000 m to be $5 \times 10^7 \text{ m}$ and the average value of $1/\tan\theta$ to be 400 means that the contribution of the geothermal buoyancy flux to the diapycnal volume transport is

$$\int \frac{G}{b_z} \frac{1}{\tan\theta} dc \approx 4 \times 10^6 \text{ m}^3 \text{ s}^{-1} = 4 \text{ Sv}, \quad (5)$$

an estimate that is consistent with that deduced by de Lavergne et al. (2016). The contribution of geothermal heating to \mathcal{E}_{BBL} is expected to grow from zero at the very densest buoyancy to no more than about 4 Sv ($1 \text{ Sv} \equiv 10^6 \text{ m}^3 \text{ s}^{-1}$) at a buoyancy appropriate to an average depth

of 2000 m. In the rest of this paper we will ignore the contribution of the geothermal heat flux to the abyssal circulation; if the geothermal heat flux were to be included, the real diapycnal transports \mathcal{E}_{BBL} (and \mathcal{E}_{net}) would be larger by amounts that vary from zero to about 4 Sv from the deepest part of the ocean up to 2000 m.

Not all of the energy that arises from the internal tide flowing over rough topography is dissipated locally, and it must be recognized that there is a background internal gravity wave field that partakes in intermittent breaking events. Observationally it seems that away from rough topography the interior ocean can be regarded as having a background diapycnal diffusivity of order $10^{-5} \text{ m}^2 \text{ s}^{-1}$, independent of height (Waterhouse et al. 2014). Taking the area of the ocean at a depth of 2000 m to be $2.5 \times 10^{14} \text{ m}^2$ and the square of the buoyancy frequency at this depth to be $N^2 = b_z \approx 2 \times 10^{-6} \text{ s}^{-2}$ means that the background diapycnal diffusivity of $10^{-5} \text{ m}^2 \text{ s}^{-1}$ contributes $\delta F = 5 \times 10^3 \text{ m}^4 \text{ s}^{-3}$ to the area-integrated diapycnal buoyancy flux F through the buoyancy surface corresponding to this depth. The vertical length scale b_z/b_{zz} at this depth is about 1000 m (this can be deduced from the slope of Fig. 3c at $b \approx 3.5 \times 10^{-3} \text{ m s}^{-2}$, corresponding to a depth of 2000 m), and the proportional change in the area of the ocean with buoyancy is not the dominant effect at this height [see Fig. 10 of Ferrari et al. (2016)] so that the contribution of the spatially constant diapycnal diffusivity $10^{-5} \text{ m}^2 \text{ s}^{-1}$ to the net diapycnal upwelling volume flux at 2000 m is $\delta \mathcal{E}_{\text{net}} = d\delta F/db = 5 \times 10^3 \text{ m}^4 \text{ s}^{-3}/(1000 \text{ m} \times 2 \times 10^{-6} \text{ s}^{-2}) = 2.5 \text{ Sv}$. From Eq. (2), with \mathcal{B}_0/b_z being the diapycnal diffusivity $10^{-5} \text{ m}^2 \text{ s}^{-1}$ and again taking $1/\tan\theta$ to be 400 and with the perimeter of the global ocean at a depth of 2000 m being $5 \times 10^7 \text{ m}$, we find that the contribution of this background diapycnal diffusivity to \mathcal{E}_{BBL} to be 0.2 Sv at a depth of 2000 m. That is, of the 2.5 Sv of extra diapycnal upwelling at 2000 m attributable to the background diapycnal diffusivity $10^{-5} \text{ m}^2 \text{ s}^{-1}$, 2.3 Sv is in the ocean interior and 0.2 Sv is upwelling in the boundary layer.

Combining the influence of geothermal heating and of the constant interior diapycnal diffusivity of $10^{-5} \text{ m}^2 \text{ s}^{-1}$, these two processes are estimated to give rise to a contribution of up to $4 + 2.5 \text{ Sv} \approx 6.5 \text{ Sv}$ to \mathcal{E}_{net} of which $4 + 0.2 \text{ Sv} \approx 4.2 \text{ Sv}$ upwells as part of \mathcal{E}_{BBL} in the BBL and the balance 2.3 Sv upwells in the ocean interior. In what follows we will ignore these contributions to the abyssal diapycnal circulation so that the real diapycnal transports \mathcal{E}_{BBL} and \mathcal{E}_{net} will be larger by amounts that vary from zero (for the densest density class) to these approximate values at 2000 m compared with the transports discussed below.

In the remainder of this paper we will take $F = \iint \mathcal{B}(b, x, y) dx dy$ to exclude the contribution of

the weak background diapycnal diffusivity (of order $10^{-5} \text{ m}^2 \text{ s}^{-1}$) to the area-integrated diffusive buoyancy flux on a buoyancy surface, and we take \mathcal{E}_{net} to exclude the contributions to the net upwelling volume flux across buoyancy surfaces from both the background diapycnal diffusivity and the geothermal heat flux. In addition, we ignore the contribution of cabbeling and thermobaricity to the diapycnal volume transport.

4. Relating the interior downwelling volume flux to the area-integrated buoyancy flux

The equation for the dianeutral velocity e in the stratified interior ocean can be found by taking the appropriate linear combination of the conservation equations for Absolute Salinity and Conservative Temperature [see McDougall (1984) or Eq. (A.22.4) of IOC et al. (2010)]. Ignoring various terms that arise from the nonlinear nature of the equation of state of seawater, the dianeutral velocity can be expressed as (subscripts denote differentiation)

$$eb_z = \mathcal{B}_z, \quad \text{or} \quad e = \frac{\mathcal{B}_z}{b_z} = \frac{\partial \mathcal{B}}{\partial b} \Big|_{x,y}. \quad (6)$$

As explained in appendix A.22 of IOC et al. (2010), this equation is the evolution equation for the locally referenced potential density; it is also the classic diapycnal advection–diffusion balance. In deriving this expression, the curvature of the buoyancy surfaces in space has been neglected, so this expression is accurate when the buoyancy surfaces are relatively flat, such as in the stratified ocean interior. Note that this expression for the diapycnal velocity applies even when the flow is unsteady, and it applies locally on any individual water column. In Eq. (6) both \mathcal{B}_z and b_z are evaluated on a vertical cast at constant x and y , so that the diapycnal velocity e is the exactly vertical component of the velocity that penetrates through the (possibly moving) buoyancy surface.

We now spatially integrate this expression for the dianeutral velocity over the buoyancy surface in the SML, that is, over that part of the area of the buoyancy surface that excludes the BBL, to evaluate the diapycnal volume flux \mathcal{E}_{SML} (defined positive upward, so that in the SML both e and \mathcal{E}_{SML} are negative) as

$$\mathcal{E}_{\text{SML}} = \iint e dx dy = \iint \frac{\mathcal{B}_z(b, x, y)}{b_z} dx dy. \quad (7)$$

It is now helpful to assume that the vertical shape of the turbulent buoyancy flux profile is exponential (see

Fig. 1), so that the variation of \mathcal{B} along the area of the buoyancy surface b in the stratified ocean interior is given by

$$\mathcal{B}(b, x, y) = \mathcal{B}_0(x, y) \exp\left(-\frac{z'}{d}\right), \quad (8)$$

where the magnitude of the diffusive buoyancy flux at the top of the BBL \mathcal{B}_0 is specified as a function of latitude and longitude $\mathcal{B}_0(x, y)$, and z' is the height of the b buoyancy surface above the top of the turbulent BBL at a given latitude and longitude. From Eqs. (6) and (8), we see that the diapycnal velocity $e(b, x, y) = \mathcal{B}_z/b_z$ on buoyancy surface b at a general latitude and longitude is

$$e(b, x, y) = -\frac{\mathcal{B}_0(x, y)}{b_z d} \exp\left(-\frac{z'}{d}\right) = -\frac{\mathcal{B}(b, x, y)}{b_z d}, \quad (9)$$

whose integral over the buoyancy surface in the SML is

$$\mathcal{E}_{\text{SML}} = - \iint \frac{\mathcal{B}(b, x, y)}{b_z d} dx dy. \quad (10)$$

In the absence of knowledge of any spatial correlation between the variations of $\mathcal{B}(b, x, y)$ and $b_z d$ along the buoyancy surface in the SML, we take the vertical scale height d to be the fixed vertical scale $d = 500$ m, and we approximate the right-hand side of Eq. (10) as

$$\mathcal{E}_{\text{SML}} \approx -\frac{F}{\langle b_z \rangle d}, \quad (11)$$

where $\langle b_z \rangle$ is the average value of b_z along the whole area of the buoyancy surface (alternatively, this area average could be performed only in the SML). This approximation to Eq. (10) is equivalent to ignoring any spatial correlation between the mixing intensity $\mathcal{B}(b, x, y)$ and the e -folding vertical buoyancy difference $\Delta b = b_z d$ over the SML on the buoyancy surface. If such a correlation exists, it is probably in the sense of reducing the magnitude of the right-hand side of Eq. (11) since we might expect that the largest values of $\mathcal{B}(b, x, y)$ on the SML would occur where the buoyancy surface is shallowest and b_z is probably also the largest. We note in passing that if we were justified in assuming that the vertical decrease in the magnitude of the buoyancy flux was an exponential function of buoyancy [rather than of height as in Eq. (8) above] so that $\mathcal{B}(b, x, y) = \mathcal{B}_0(x, y) \exp[-(b - b_0)/\Delta b]$, where the e -folding buoyancy scale Δb is constant along the buoyancy surface, then \mathcal{E}_{SML} would be given by $\mathcal{E}_{\text{SML}} = -F/\Delta b$ so that \mathcal{E}_{SML} and F would simply be proportional to each other. But we are not aware of any observational support for the e -folding buoyancy scale Δb being spatially invariant, so we

follow the conventional practice of adopting an e -folding scale in height, that is, we retain the form equation (8).

If the magnitude of the buoyancy flux $\mathcal{B}(b, x, y)$ of Eq. (8) were taken to be a linear function of z' , varying from $\mathcal{B}_0(x, y)$ at $z' = 0$ to zero at $z' = d$, then the right-hand side of Eq. (11) would be approximately doubled so that $\mathcal{E}_{\text{SML}} = -2F/(\langle b_z \rangle d)$.

This rather direct relationship, Eq. (11), between the downwelling volume transport \mathcal{E}_{SML} in the SML and the magnitude of the area-integrated interior buoyancy flux F is a direct result of the relationship between the diapycnal velocity and the diffusive buoyancy flux of Eqs. (6) and (8), namely, $eb_z = \mathcal{B}_z = -\mathcal{B}/d$. Note that the vertical scale height d in the above equations can be defined as $d = -\mathcal{B}/\mathcal{B}_z$, rather than having to assume an exponential vertical profile, and similar results would follow. Thus, the choice of an exponential profile is one of analytical convenience.

Just like our expressions (2) and (3) for the net diapycnal volume flux in the BBL, the net diapycnal volume flux [Eq. (11)] for the SML near-boundary diapycnal volume flux applies to a local area integral along a buoyancy surface, and it applies even when the flow is unsteady with vertical heaving motion and with a mean epineutral transport between pairs of buoyancy surfaces.

5. The diapycnal upwelling in the BBL as a vertical integral of the net global diapycnal upwelling

Recalling that we are ignoring the geothermal heat flux, the complete buoyancy budget [Eq. (3)] $\mathcal{E}_{\text{net}} = dF/db$ can be integrated with respect to buoyancy,

$$F = \int_{b_{\text{min}}}^b \mathcal{E}_{\text{net}} db', \quad (12)$$

yielding a convenient expression for the area-integrated diffusive buoyancy budget F , where $\mathcal{E}_{\text{net}} = \mathcal{E}_{\text{BBL}} + \mathcal{E}_{\text{SML}}$ is the net diapycnal upwelling transport through both the BBL and the SML, and the definite integral is performed from the very densest water with buoyancy b_{min} . In appendix B, it is shown that this expression for F [Eq. (12)] is equivalent to the volume-integrated buoyancy budget [Eq. (B1)] for the volume that is less buoyant than the buoyancy value b in the global ocean in steady state.

Substituting this expression for F into Eq. (11) gives

$$\mathcal{E}_{\text{SML}} \approx -\frac{1}{\langle b_z \rangle d} \int_{b_{\text{min}}}^b \mathcal{E}_{\text{net}} db'. \quad (13)$$

The lower limit of the integration here is the least buoyant (densest) water in the World Ocean, where

F (and hence \mathcal{E}_{SML}) is zero since the area of this densest surface tends to zero.

Equation (13) is the key result of this paper; it states that knowledge in the abyssal ocean of (i) the stratification (b_z), (ii) the vertical e -folding length scale of the diffusive buoyancy flux d , and (iii) the net upwelling of AABW as a function of buoyancy $\mathcal{E}_{\text{net}}(b)$ yields an estimate of the sinking diapycnal volume flux \mathcal{E}_{SML} in the ocean interior.

The diapycnal volume flux in the BBL follows from Eq. (13) and the volume conservation equation $\mathcal{E}_{\text{net}} = \mathcal{E}_{\text{BBL}} + \mathcal{E}_{\text{SML}}$, so that

$$\mathcal{E}_{\text{BBL}} \approx \mathcal{E}_{\text{net}} + \frac{1}{\langle b_z \rangle d} \int_{b_{\text{min}}}^b \mathcal{E}_{\text{net}} db'. \quad (14)$$

As an initial demonstration of these equations, in this paragraph we will assume that the net upwelling volume flux \mathcal{E}_{net} is independent of height (buoyancy) in the abyss and define buoyancy (ms^{-2}) with respect to a neutral density value of 28.3 kg m^{-3} as

$$b = 0.01(28.3 - \gamma), \quad (15)$$

where γ is neutral density (kg m^{-3}) (Jackett and McDougall 1997). We will assume that the buoyancy value $b_{\text{min}} = 0 \text{ ms}^{-2}$ characterizes the densest water in the World Ocean. At a depth of 2500 m, ocean atlases show that $\gamma \approx 28.05 \text{ kg m}^{-3}$, $b \approx 2.5 \times 10^{-3} \text{ ms}^{-2}$, $b_z \approx 10^{-6} \text{ s}^{-2}$, and taking d to be 500 m, Eqs. (13) and (14) yield $\mathcal{E}_{\text{SML}} \approx -5\mathcal{E}_{\text{net}}$ and $\mathcal{E}_{\text{BBL}} \approx 6\mathcal{E}_{\text{net}}$. In this way, if \mathcal{E}_{net} were say 18 Sv then the diapycnal transport in the BBL would be about 108 Sv while the downwelling in the interior SML would be 90 Sv.

If instead of assuming that \mathcal{E}_{net} is independent of height (buoyancy) in the abyss, we take it to be a linearly increasing function of buoyancy as suggested by the model studies of Ferrari et al. (2016), then the above ratio of \mathcal{E}_{SML} to \mathcal{E}_{net} becomes $\mathcal{E}_{\text{SML}} \approx -2.5\mathcal{E}_{\text{net}}$, closer to the values of approximately -1.5 seen in Fig. 7 of Ferrari et al. (2016). The remaining discrepancy could be due to the model runs having a larger stratification ($\langle b_z \rangle$) than the observations or due to the correlation along isopycnals in the SML between the mixing intensity $\mathcal{B}(b, x, y)$ and the vertical stratification b_z in Eq. (10). The ratio $|\mathcal{E}_{\text{SML}}|/\mathcal{E}_{\text{net}}$ in Fig. 9 of Ferrari et al. (2016) is based on applying the Nikurashin and Ferrari (2013) estimate of mixing induced by breaking topographic waves and is slightly larger at about $|\mathcal{E}_{\text{SML}}|/\mathcal{E}_{\text{net}} \approx 2$ (and hence $\mathcal{E}_{\text{BBL}}/\mathcal{E}_{\text{net}} \approx 3$) in the abyss.

In an attempt to be a little more oceanographically realistic, we have constructed a specific function of \mathcal{E}_{net} as a function of buoyancy based on Fig. 2a of Lumpkin and Speer (2007):

$$\mathcal{E}_{\text{net}} = C \left(1 - \frac{b}{B}\right) \left[1 - \exp\left(-\frac{b}{A}\right)\right], \quad (16)$$

where $C = 25.7 \times 10^6 \text{ m}^3 \text{ s}^{-1}$, $B = 7 \times 10^{-3} \text{ ms}^{-2}$, and $A = 6.8 \times 10^{-4} \text{ ms}^{-2}$ [and using the relationship between buoyancy and neutral density is given by Eq. (15)]. This function has \mathcal{E}_{net} equal to zero at $b_{\text{min}} = 0 \text{ ms}^{-2}$ and rises to a maximum value of $\mathcal{E}_{\text{net}} = 18 \text{ Sv}$ at $b = 1.5 \times 10^{-3} \text{ ms}^{-2}$, which corresponds to a depth of approximately 3000 m. This functional form [Eq. (16)] for $\mathcal{E}_{\text{net}}(b)$ is illustrated in Fig. 3a, and its integral $F = \int_0^b \mathcal{E}_{\text{net}} db'$ is shown in Fig. 3b. The next panel in Fig. 3 shows the reciprocal of the area-averaged values of $\langle b_z \rangle$ as a function of b using the hydrographic data of Gouretski and Koltermann (2004), which we have labeled with neutral density γ . Figure 3d shows the magnitude of the right-hand side of Eq. (13) $|\mathcal{E}_{\text{SML}}|$, obtained by multiplying Figs. 3b and 3c and dividing by $d = 500 \text{ m}$. Also shown in Fig. 3d is $\mathcal{E}_{\text{BBL}} = \mathcal{E}_{\text{net}} + |\mathcal{E}_{\text{SML}}|$ and \mathcal{E}_{net} itself. The ratios $\mathcal{E}_{\text{BBL}}/\mathcal{E}_{\text{net}}$ and $|\mathcal{E}_{\text{SML}}|/\mathcal{E}_{\text{net}}$ are shown in Fig. 3e. The horizontal b axis in Fig. 3 ranges from zero up to $5 \times 10^{-3} \text{ ms}^{-2}$ but the upper limit of the abyssal ocean, corresponding to a depth of $\sim 2000 \text{ m}$, is at approximately $b = 3.5 \times 10^{-3} \text{ ms}^{-2}$ ($\gamma \approx 27.95 \text{ kg m}^{-3}$).

From Fig. 3 we see that while we have taken the maximum value of the net upward diapycnal transport to be 18 Sv, the maximum diapycnal upwelling in the BBL is 103 Sv and the downwelling in the interior SML is as large as 86 Sv. According to our discussion near the end of section 3, the inclusion of (i) geothermal heating and (ii) weak interior mixing with a diapycnal diffusivity of $10^{-5} \text{ m}^2 \text{ s}^{-1}$ adds a transport that increases from zero at the seafloor to 4.2 Sv at 2000 m ($\gamma \approx 27.95 \text{ kg m}^{-3}$ and $b = 3.5 \times 10^{-3} \text{ ms}^{-2}$) to \mathcal{E}_{BBL} . The corresponding change to \mathcal{E}_{SML} increases from zero at the seafloor to 2.3 Sv at 2000 m, thus making \mathcal{E}_{SML} slightly less negative. It is clear that while both geothermal heating and weak background interior diffusion make an appreciable contribution to the net transport \mathcal{E}_{net} (of up to 35%), neither geothermal heating nor weak background interior diffusion makes a material contribution to \mathcal{E}_{BBL} or \mathcal{E}_{SML} individually.

In much of the abyssal ocean we have found that the upwelling diapycnal transport in the BBL \mathcal{E}_{BBL} is approximately 5 times the net upwelling of AABW \mathcal{E}_{net} (Fig. 3e in the range $10^{-3} < b < 3.5 \times 10^{-3} \text{ ms}^{-2}$ or $27.95 < \gamma < 28.2 \text{ kg m}^{-3}$, which corresponds approximately to the height range $-3500 < z < -2000 \text{ m}$). Such a large amplification factor describing strong recirculation of abyssal water seems surprising, but it is broadly consistent with the model findings of Ferrari et al. (2016), depending mainly on how \mathcal{E}_{net} varies with buoyancy in the abyss. If in the real ocean each

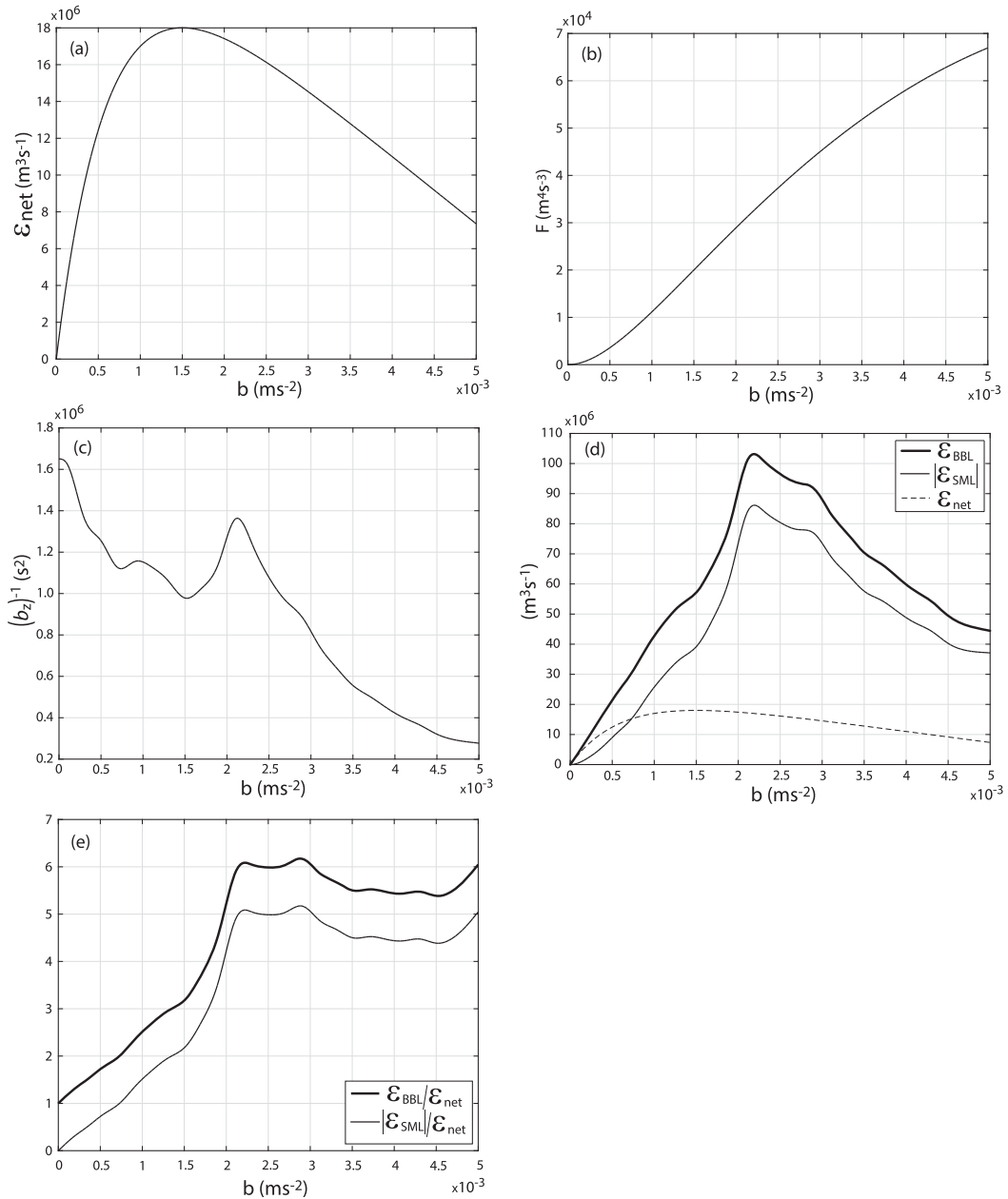


FIG. 3. (a) The net upwelling transport \mathcal{E}_{net} of Eq. (16) as a function of buoyancy b (m s^{-2}) defined in terms of neutral density γ (kg m^{-3}) by $b = 0.01(28.3 - \gamma)$. (b) The magnitude of the area-integrated diffusive buoyancy flux F , as estimated as the buoyancy integral $F = \int_0^b \mathcal{E}_{\text{net}} db'$ of (a). (c) The reciprocal of the area-averaged values of $\langle b_z \rangle$ as a function of b from the hydrographic data of Gouretski and Koltermann (2004). (d) The diapycnal volume transport $|\mathcal{E}_{\text{SML}}|$ evaluated from Eq. (13) as essentially the product of panels (b) and (c). Also shown are \mathcal{E}_{BBL} from Eq. (14), and \mathcal{E}_{net} is repeated from (a). (e) The ratios $\mathcal{E}_{\text{BBL}}/\mathcal{E}_{\text{net}}$ and $|\mathcal{E}_{\text{SML}}|/\mathcal{E}_{\text{net}}$ as a function of buoyancy.

descending plume of AABW sinks all the way to the densest part of the ocean without significant entrainment or detrainment, then \mathcal{E}_{net} will be independent of buoyancy. If the sinking plumes of AABW entrain fluid from the environment all the way to the seafloor, then \mathcal{E}_{net} will be a decreasing function of buoyancy. If, on the

other hand, the sinking plumes of AABW detrain substantially above the bottom (a la Baines 2005) or if there are multiple sources of AABW of different densities, then \mathcal{E}_{net} will increase with buoyancy in the deepest part of the ocean, as found in the Ferrari et al. (2016) model study.

What aspect of our development could lead to an overestimate of this BBL upwelling amplification ratio $\mathcal{E}_{\text{BBL}}/\mathcal{E}_{\text{net}}$? We see two possibilities. First, it is possible that the assumed vertical e -folding scale $d = 500$ m is too small. The second uncertainty is the possible correlation along isopycnals in the SML between the magnitude of the buoyancy flux per unit area $\mathcal{B}(b, x, y)$ and the e -folding vertical buoyancy difference $\Delta b = b_z d$ in Eq. (10).

The strong upwelling (of up to 100 Sv) in the BBL in the abyssal ocean, being approximately 5 times the net upwelling of ABBW, is confined to the turbulent boundary layer whose vertical extent is h and whose horizontal extent is $h/\tan\theta$. With $h \approx 50$ m and with $\tan\theta \approx 1/400$, this horizontal distance over which the very strong upwelling of ~ 100 Sv occurs is no wider than 20 km or about 0.2° of longitude or latitude, as is sketched in Fig. 4.

The strong diapycnal downwelling (of as much as 86 Sv) is confined to the stratified ocean interior that is mostly between h and $2d + h$ above the seafloor. This region extends from $h/\tan\theta$ to $(2d + h)/\tan\theta$ away from the continental boundaries. The width of this horizontal region is $2d/\tan\theta$, and with $d \approx 500$ m and $\tan\theta \approx 1/400$, this horizontal distance over which the strong downwelling occurs is no wider than 400 km or 4° of longitude or latitude, with the magnitude of the downwelling velocity decreasing away from the boundary toward the ocean interior.

What is the magnitude of the near-boundary diapycnal diffusivity needed to upwell ~ 100 Sv through isopycnals in the BBL? From Eq. (2), we see that

$$\mathcal{E}_{\text{BBL}} = \int \frac{\mathcal{B}_0}{b_z} \frac{1}{\tan\theta} dc = \int \frac{D_0}{\tan\theta} dc, \quad (17)$$

where we have ignored the contribution of the geothermal heat flux to \mathcal{E}_{BBL} , and we have introduced the diapycnal diffusivity $D_0 = \mathcal{B}_0/b_z$ in the stratified ocean just above the BBL. Taking the perimeter of the global ocean at this depth to be 5×10^7 m and the average value of $1/\tan\theta$ to be 400 means that in order to upwell $\mathcal{E}_{\text{BBL}} = 100$ Sv in the BBL requires the turbulent diffusivity immediately above the BBL to be approximately $D_0 \approx 5 \times 10^{-3} \text{ m}^2 \text{ s}^{-1}$. This is a large diapycnal diffusivity, especially given that it represents the average value along an in-crop line, thus requiring even larger values in the locations where the mixing intensity is largest (near rough topography). The required diapycnal diffusivity would be reduced if the e -folding vertical length scale is significantly greater than 500 m or if there is a significant correlation [see Eq. (10)] between the mixing intensity $\mathcal{B}(b, x, y)$ and the vertical stratification b_z along buoyancy surfaces.

With $O(100)$ Sv of upwelling in the BBL and the almost balancing downwelling in the SML, the average vertical component of the diapycnal velocities would be $O(10^{-4})$ and $O(-5 \times 10^{-6}) \text{ m s}^{-1}$, respectively, in the BBL and SML based on the perimeter of the global ocean being 5×10^7 m and the appropriate horizontal widths of the BBL and SML being 20 and 400 km, respectively.

The physical process that causes both the diapycnal volume fluxes \mathcal{E}_{BBL} and \mathcal{E}_{SML} is the turbulent diapycnal diffusive buoyancy flux [see Eqs. (2)–(4)], while Eq. (13) is diagnostic in nature since it is written in terms of the net diapycnal upwelling rate \mathcal{E}_{net} rather than in terms of the diffusive buoyancy flux. This diagnostic equation has made use of the steady-state buoyancy budget, which requires the interior density stratification to be consistent with the area-integrated turbulent diapycnal buoyancy flux $F = \int_0^b \mathcal{E}_{\text{net}} db'$ and its derivative dF/db . The use of this overall buoyancy budget in the expressions for the diapycnal volume fluxes is the key simplifying feature that has led to Eq. (13) and the results of Fig. 3. Because of this use of F in terms of \mathcal{E}_{net} , we have not needed to specify the processes that contribute to the area-integrated diffusive buoyancy flux or its buoyancy derivative dF/db . This variation of the magnitude of the area-integrated diffusive buoyancy flux with buoyancy can be due to (i) the vertical variation of the area available for mixing and/or (ii) it can be due to the values of \mathcal{B}_0 at the top of the BBL varying vertically with buoyancy along the sloping seafloor. In the following sections we will discuss some specific geometries in which we can readily calculate F and dF/db , thereby evaluating all three diapycnal transports \mathcal{E}_{net} , \mathcal{E}_{SML} , and \mathcal{E}_{BBL} .

In the following four sections we move beyond the diagnostic relationships [Eqs. (13) and (14)] and derive expressions for the upwelling and downwelling volume fluxes in terms of the mixing intensity \mathcal{B}_0 in oceans of different geometry.

6. A two-dimensional global ocean

The first example we consider is where the mixing occurs on a continental boundary that is two-dimensional in the sense that the length of the perimeter where an isopycnal intersects the continent is constant, that is, it is the same length over a range of densities. We also restrict attention to the case where the slope of the sea floor $\tan\theta$ is constant. In this case we may simplify the expressions (1) and (4) for F and \mathcal{E}_{SML} , respectively, and we are able to show that the mixing activity just above the BBL must increase with buoyancy in order to achieve a net positive upwelling.

In this two-dimensional situation we take the x coordinate to be in the horizontal direction, and y is the coordinate into the page, so to speak; in Fig. 2 we may take x to be to the right and y into the page. The magnitude of the buoyancy flux at the top of the BBL can be expressed as a function of latitude and longitude $\mathcal{B}_0(x, y)$ or as a function $\mathcal{B}_0(b, y)$ of buoyancy and the distance y into the page along the boundary at the top of the turbulent boundary layer. The value of $\mathcal{B}_0(x, y)$ at a distance x from the point a on Fig. 2 is now expressed as the first two terms in a Taylor series expansion about point a where the buoyancy has the value b_0 so that (with z' being the height above the top of the turbulent boundary layer at a given horizontal location and noting that $z' = x \tan\theta$)

$$\begin{aligned} \mathcal{B}_0(x, y) &\approx \mathcal{B}_0(b_0, y) - (\mathcal{B}_0)_b b_z z' \\ &= \mathcal{B}_0(b_0, y) - (\mathcal{B}_0)_b b_z x \tan\theta. \end{aligned} \quad (18)$$

The magnitude of the buoyancy flux at a general location on the b buoyancy surface is

$$\mathcal{B}(b, x, y) \approx [\mathcal{B}_0(b_0, y) - (\mathcal{B}_0)_b b_z x \tan\theta] \exp\left(-\frac{z'}{d}\right), \quad (19)$$

while along the isopycnal surface the area-integrated value of \mathcal{B} is given by

$$\begin{aligned} F &= \iint \mathcal{B} dx dy \\ &= \iint [\mathcal{B}_0 - (\mathcal{B}_0)_b b_z x \tan\theta] \exp\left(-\frac{x \tan\theta}{d}\right) dx dy, \end{aligned} \quad (20)$$

where $\mathcal{B}_0(b_0, y)$ has been replaced by \mathcal{B}_0 for notational convenience.

We now turn our attention to forming the expression for the downwelling volume transport across the interior part of the isopycnal \mathcal{E}_{SML} . The diapycnal velocity on an isopycnal that is in the stratified ocean interior is [from Eq. (6), i.e., $eb_z = \mathcal{B}_z$ and using Eq. (19)]

$$e(b, x, y) = -\frac{[\mathcal{B}_0 - (\mathcal{B}_0)_b b_z x \tan\theta]}{b_z d} \exp\left(-\frac{z'}{d}\right), \quad (21)$$

and taking the area integral of this on the isopycnal gives

$$\mathcal{E}_{\text{SML}} = -\iint \left[\frac{\mathcal{B}_0}{b_z d} - (\mathcal{B}_0)_b \frac{x \tan\theta}{d} \right] \exp\left(-\frac{x \tan\theta}{d}\right) dx dy. \quad (22)$$

Taking $b_z d$ to be constant over the isopycnal and then comparing Eqs. (20) and (22) confirms our previously derived relationship [Eq. (11)], namely, that $\mathcal{E}_{\text{SML}} = -F/(b_z d)$.

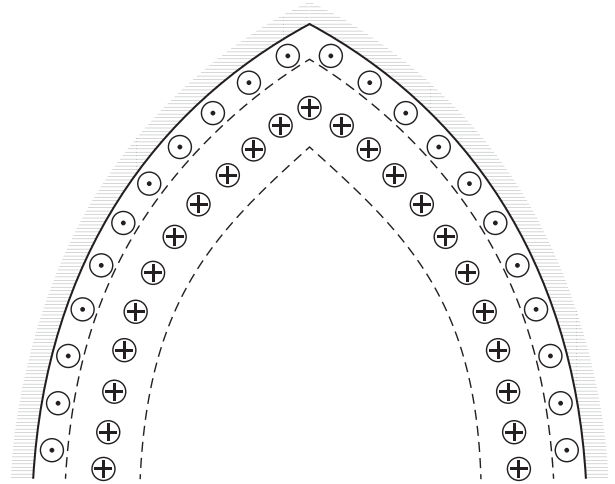


FIG. 4. Sketch of the spatial distribution of the intense upwelling hard up against the boundary (arrow point in circle) and downwelling (the crossed feathers at the trailing end of the arrow inside the circles) in a canonical Northern Hemisphere ocean. The interior of each isopycnal has no diapycnal motion while there is downwelling only within approximately 4° (~ 400 km) of the boundary and very strong upwelling within just 0.2° (~ 20 km) of the continental boundaries. With $O(100)$ Sv of upwelling in the BBL and downwelling in the SML, the average vertical component of the diapycnal velocities would be $O(10^{-4})$ and $O(-5 \times 10^{-6})$ m s^{-1} in the BBL and SML, respectively.

In this two-dimensional geometry, the x integration can be performed independently of the y integration, and integrating over x from zero to infinity and using the two integral relations $\int_0^\infty \exp(-s) ds = 1$ and $\int_0^\infty s \exp(-s) ds = 1$, we find [from Eqs. (20) and (22)] F and \mathcal{E}_{SML} to be

$$F = \int \mathcal{B}_0 \frac{d}{\tan\theta} dy - \int (\mathcal{B}_0)_b b_z d \frac{d}{\tan\theta} dy, \quad 2\text{-dim}, \quad (23)$$

and

$$\mathcal{E}_{\text{SML}} = -\int \frac{\mathcal{B}_0}{b_z} \frac{1}{\tan\theta} dy + \int (\mathcal{B}_0)_b \frac{d}{\tan\theta} dy. \quad 2\text{-dim}. \quad (24)$$

The effective horizontal area on an isopycnal in this two-dimensional situation where the diapycnal diffusion is significant is proportional to $\int (d/\tan\theta) dy$, and since $d/\tan\theta$ is taken to be independent of buoyancy, the area of significant diffusive buoyancy flux is also independent of buoyancy, that is, constant with height. Note that the total area of the isopycnal will increase with height whenever the ocean does not have vertical sidewalls, but what is relevant for the buoyancy budget is the area of active mixing in the SML and whether that area increases with buoyancy or not.

In this two-dimensional situation we are able to be quite specific about the spatial variation of the diffusive buoyancy flux that is needed to achieve net upwelling \mathcal{E}_{net} . The first part of the right-hand side of Eq. (24) is equal to $-\mathcal{E}_{\text{BBL}}$ [see the general expression for \mathcal{E}_{BBL} of Eq. (2)] so that in this two-dimensional situation we find from Eq. (24) that \mathcal{E}_{net} is given by (using $\mathcal{E}_{\text{net}} = \mathcal{E}_{\text{BBL}} + \mathcal{E}_{\text{SML}}$)

$$\mathcal{E}_{\text{net}} = \int (\mathcal{B}_0)_b \frac{d}{\tan\theta} dy. \quad 2\text{-dim.} \quad (25)$$

This shows that in order for upwelling of bottom water to be possible in this two-dimensional situation, the magnitude of the diffusive buoyancy flux at the top of the boundary layer \mathcal{B}_0 must increase with buoyancy (or height). That is, in this two-dimensional situation in which both the distance into the page and the sea floor slope $\tan\theta$ are independent of height, then $(\mathcal{B}_0)_b$ being positive is the only way that the magnitude of the diffusive buoyancy flux F can increase with buoyancy, thus allowing $dF/db = \mathcal{E}_{\text{net}}$ to be positive. One way that $(\mathcal{B}_0)_b$ can be positive is if the near-boundary turbulent diffusivity D_0 is constant and the vertical stratification b_z increases in the vertical, that is, if $b_{zz} > 0$.

The two-dimensional geometry of this section, in which properties are independent of the coordinate into the page, is the one considered by Thorpe (1987) and Garrett (1990, 2001). These authors also imposed the diffusive buoyancy flux to be the same across each isopycnal [in our terminology, $(\mathcal{B}_0)_b = 0$], and hence our result that there is no net upwelling in this situation is consistent with their result that the net upwelling per unit distance into the page is $D_\infty/\tan\theta$, since in our case the diffusivity far from the boundary D_∞ is zero.

7. A conical global ocean with constant \mathcal{B}_0

Next we consider a different example where (i) the magnitude of the buoyancy flux per unit area at the top of the BBL $\mathcal{B}_0(x, y)$ is independent of latitude and longitude so that it is simply the constant value \mathcal{B}_0 and $(\mathcal{B}_0)_b = 0$, (ii) the ocean topography is a cone whose surface of revolution makes a constant angle θ to the horizontal, and (iii) the interior stratification b_z is constant along each isopycnal. The upward flow in the BBL is still given by Eq. (2), which in this geometry is

$$\mathcal{E}_{\text{BBL}} = \int \frac{\mathcal{B}_0}{b_z} \frac{1}{\tan\theta} dc = 2\pi\mathcal{B}_0 \frac{R}{b_z \tan\theta} \quad \text{conical ocean,} \quad (26)$$

where R is the radius of the cone at the top of the BBL on this buoyancy surface. The area-integrated value of \mathcal{B} on the isopycnal is

$$\begin{aligned} F &= 2\pi\mathcal{B}_0 \int_0^R r \exp\left[-\frac{(R-r)\tan\theta}{d}\right] dr \\ &= 2\pi\mathcal{B}_0 \left(\frac{d}{\tan\theta}\right)^2 \left[\frac{R\tan\theta}{d} - 1 + \exp\left(-\frac{R\tan\theta}{d}\right)\right] \\ &\quad \text{conical ocean,} \end{aligned} \quad (27)$$

and the value of \mathcal{E}_{SML} is $-F/(b_z d)$. The net upwelling \mathcal{E}_{net} is dF/db , which can be evaluated by differentiating Eq. (27) using $dF/db = F_R R_z / b_z$ and using the geometry of the conical ocean, which means that $R_z = 1/\tan\theta$. This reasoning leads to

$$\begin{aligned} \mathcal{E}_{\text{net}} &= \frac{dF}{db} = 2\pi\mathcal{B}_0 \frac{d}{b_z (\tan\theta)^2} \\ &\quad \times \left[1 - \exp\left(-\frac{R\tan\theta}{d}\right)\right] \quad \text{conical ocean.} \end{aligned} \quad (28)$$

This value of \mathcal{E}_{net} agrees with calculating it as $\mathcal{E}_{\text{BBL}} + \mathcal{E}_{\text{SML}}$ using the expressions above for \mathcal{E}_{BBL} and \mathcal{E}_{SML} .

This example shows that when the area of the SML region increases with buoyancy, net upwelling can occur even when \mathcal{B}_0 is constant. The value of the volume flux ratio $\mathcal{E}_{\text{BBL}}/\mathcal{E}_{\text{net}}$ for this conical ocean is given by the ratio of Eqs. (26) and (28), namely,

$$\frac{\mathcal{E}_{\text{BBL}}}{\mathcal{E}_{\text{net}}} = \frac{R\tan\theta/d}{[1 - \exp(-R\tan\theta/d)]}, \quad \text{conical ocean,} \quad (29)$$

and if the radius R is significantly larger than $d/\tan\theta$ then this equation can be approximated as $\mathcal{E}_{\text{BBL}}/\mathcal{E}_{\text{net}} \approx R\tan\theta/d$. In this limit of $R \gg d/\tan\theta$, \mathcal{E}_{BBL} is much larger than \mathcal{E}_{net} , and [from Eq. (28)] the net upwelling of bottom water \mathcal{E}_{net} is independent of the radius R of the cone and so is independent of buoyancy. That is, the same net volume flux \mathcal{E}_{net} upwells through all height levels of the conical ocean. By contrast, both \mathcal{E}_{BBL} and $|\mathcal{E}_{\text{SML}}|$ increase linearly with R , that is, increase linearly with height (see Fig. 5).

8. A generic seamount

We return here to consider the nonglobal, nonsteady situation of Fig. 2 in the specific case of a seamount. We take the key feature of a seamount to be that the magnitude of the area-integrated diapycnal diffusive buoyancy flux F in the vicinity of the seamount across isopycnals that intersect the seamount is a decreasing function of height, that is, a decreasing function of buoyancy. That is, $dF/db < 0$. The reason for this is that

for a surface of revolution about the vertical axis, the interior mixing mainly occurs on an annulus of width $2d/\tan\theta$ whose radius decreases as the top of the seamount is approached. If \mathcal{B}_0 or $1/\tan\theta$ increased strongly with buoyancy, then dF/db could still be positive in this depth range for a seamount, but we consider that this would not occur over a significant depth range on a typical seamount. From Eq. (3), $\mathcal{E}_{\text{BBL}} + \mathcal{E}_{\text{SML}} = \mathcal{E}_{\text{net}} = dF/db$, which applies not just globally but also to a local region such as the region near a seamount so that we deduce that the net diapycnal volume flux \mathcal{E}_{net} in the vicinity of a seamount is expected to be downward, as first pointed out by McDougall (1989). Hence, given a certain volume flux of AABW \mathcal{E}_{BW} that needs to be upwelled across isopycnals, the continental boundary regions (including both the BBL and SML regions) must transport more than \mathcal{E}_{BW} upward across isopycnals simply to compensate for the net downward motion of that part of the ocean that surrounds those seamounts that do not rise above a depth of 2000 m.

The buoyancy budget inside the BBL implies that the flow along this BBL \mathcal{E}_{BBL} must be upward, even in the seamount case; that is, our general expression for \mathcal{E}_{BBL} [Eq. (2)] applies to the seamount situation. But the downward diapycnal flow in the stratified interior \mathcal{E}_{SML} is generally larger in magnitude than \mathcal{E}_{BBL} for a seamount. We now examine the special case of a conical seamount with a constant diffusive buoyancy flux just above the BBL.

9. A conical seamount with constant \mathcal{B}_0

Here, we consider a conical seamount where again (i) the mixing intensity at the top of the BBL is simply the constant value \mathcal{B}_0 , (ii) the seamount topography is a cone whose surface of revolution makes a constant angle θ to the horizontal, and (iii) the interior stratification b_z is constant along each isopycnal. The upward flow in the turbulent boundary layer is given by Eq. (2), which in this geometry is the same as for the conical global ocean [Eq. (26)], namely,

$$\begin{aligned} \mathcal{E}_{\text{BBL}} &= \int \frac{\mathcal{B}_0}{b_z} \frac{1}{\tan\theta} dc \\ &= 2\pi\mathcal{B}_0 \frac{R}{b_z \tan\theta}, \quad \text{conical seamount,} \end{aligned} \quad (30)$$

where R is the radius of the cone at the top of the turbulent boundary layer on this buoyancy surface, with R decreasing linearly with buoyancy. The area-integrated value of \mathcal{B} on an isopycnal is

$$\begin{aligned} F &= 2\pi\mathcal{B}_0 \int_R^\infty r \exp\left[-\frac{(r-R)\tan\theta}{d}\right] dr \\ &= 2\pi\mathcal{B}_0 \frac{Rd}{\tan\theta} + 2\pi\mathcal{B}_0 \left(\frac{d}{\tan\theta}\right)^2, \quad \text{conical seamount,} \end{aligned} \quad (31)$$

and the value of \mathcal{E}_{SML} is $-F/(db_z)$. The net upwelling of water in the vicinity of the seamount \mathcal{E}_{net} is dF/db , which can be evaluated by differentiating Eq. (31) using $dF/db = F_R R_z / b_z$ and using the geometry of the conical seamount, which means that $R_z = -1/\tan\theta$. This reasoning leads to the following expression for the net diapycnal volume flux in the vicinity of the seamount:

$$\mathcal{E}_{\text{net}} = \frac{dF}{db} = -2\pi\mathcal{B}_0 \frac{d}{b_z (\tan\theta)^2} \quad \text{conical seamount.} \quad (32)$$

This value of \mathcal{E}_{net} agrees with calculating it as $\mathcal{E}_{\text{BBL}} + \mathcal{E}_{\text{SML}}$ using the expressions above for \mathcal{E}_{BBL} and \mathcal{E}_{SML} .

This conical seamount example shows that when the area of the interior region of mixing decreases with buoyancy, net downwelling, $\mathcal{E}_{\text{net}} < 0$, occurs when \mathcal{B}_0 is constant. The ratio of the upwelling \mathcal{E}_{BBL} in the BBL surrounding the seamount to \mathcal{E}_{net} for this conical seamount is given by the ratio of Eqs. (30) and (32), namely,

$$\frac{\mathcal{E}_{\text{BBL}}}{\mathcal{E}_{\text{net}}} = -\frac{R \tan\theta}{d} \quad \text{conical seamount.} \quad (33)$$

This ratio has the same magnitude but opposite sign to the value $R \tan\theta/d$ of the conical ocean case (which applies in the limit $R \gg \tan\theta/d$). The net downwelling volume flux \mathcal{E}_{net} in the vicinity of the seamount is independent of the radius R of the cone [see Eq. (32)] and so is independent of buoyancy. That is, the same net volume flux \mathcal{E}_{net} downwells through all height levels of the cone. By contrast, both \mathcal{E}_{BBL} and $|\mathcal{E}_{\text{SML}}|$ increase linearly with R , that is, linearly with depth. This is illustrated in Fig. 6a.

Notice from Eq. (32) that the net diapycnal volume flux $|\mathcal{E}_{\text{net}}|$ is proportional to $(\tan\theta)^{-2}$ so that near the top of a realistic seamount (Fig. 6b) where the bottom slope is small, $|\mathcal{E}_{\text{net}}|$ is large and will tend to decrease toward the midheights of the seamount where the bottom slope is the largest, increasing again toward the flanks (the bottom) of the seamount where the bottom slope is again small. This would suggest that the seamount is a source of fluid at midheight but a sink for exterior fluid at other heights. That is, a realistic-shaped seamount can act as both a sink and a source of surrounding seawater at different heights, but on average, since \mathcal{E}_{net} is expected to be predominantly negative in the region of a seamount, the surrounding seawater is drawn toward the seamount near the top of

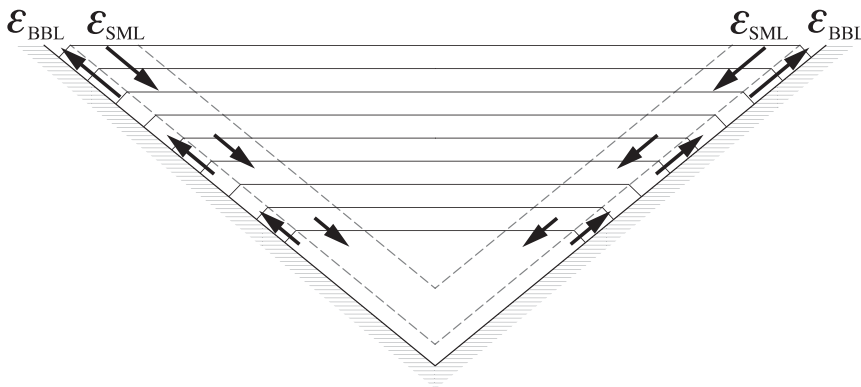


FIG. 5. Sketch of the conical ocean with a constant value of \mathcal{B}_0 at the top of the turbulent boundary layer. The upward diapycnal flow in the turbulent boundary layer \mathcal{E}_{BBL} increases with height while the downward diapycnal flow in the stratified near-seamount interior \mathcal{E}_{SML} also increases in magnitude with height. The diapycnal velocities are independent of height in both the BBL and the SML (if b_z is constant). The net upwelling \mathcal{E}_{net} in the abyssal ocean is balanced by a sinking plume of AABW that is not shown in the sketch.

the seamount and is then made less buoyant and sinks though isopycnals.

10. Requirements for global upwelling: Scaling arguments

The global ocean does have AABW rising through the abyss, and this implies that the area-integrated buoyancy flux needs to increase with buoyancy (since $\mathcal{E}_{\text{net}} = dF/db$), and here we ask what is required of the mixing intensity and the bathymetry in order to ensure that $dF/db > 0$. Since F is always positive, we examine that ratio $(F^{-1})dF/db$. The area of active mixing on each isopycnal scales as the horizontal width of the BBL and SML, $d/\tan\theta$, times the perimeter L of the topography (see Fig. 2). Hence, $F \sim \mathcal{B}_0 L d / \tan\theta$ so that $(F^{-1})dF/db$ scales as

$$\frac{1}{F} \frac{dF}{db} \sim \frac{(\mathcal{B}_0)_b}{\mathcal{B}_0} + \frac{L_b}{L} - \frac{(\tan\theta)_b}{\tan\theta} + \frac{d_b}{d}. \quad (34)$$

This indicates that there are four different ways that net upwelling can be enabled, namely, (i) if the magnitude of the buoyancy flux at the top of the BBL \mathcal{B}_0 is an increasing function of buoyancy, (ii) if the length (perimeter) L is an increasing function of buoyancy, (iii) if the slope of the seafloor $\tan\theta$ is a decreasing function of buoyancy, and (iv) if the vertical length scale d is an increasing function of buoyancy. The influence of the first three of these factors have been illustrated in the previous sections. This argument is essentially a linearization of vertical changes in the full expression (1) for the area-integrated buoyancy flux, but nevertheless, it seems useful.

11. Volume-integrated dissipation

Starting with Munk and Wunsch (1998), the strength of the overturning circulation has been related to the volume-integrated buoyancy flux generated by turbulent mixing. Here, we investigate whether the strong diapycnal upwelling along the BBL and the nearly equally strong diapycnal downwelling in the SML have important implications for the energy budget of the net overturning circulation.

The volume-integrated value of \mathcal{B} in the global ocean below 2000 m is calculated using the definition [Eq. (1)] of F , which is the area integral of \mathcal{B} along an isopycnal, excluding regions of dense water formation:

$$\begin{aligned} \mathcal{G} &= \iiint \mathcal{B} dx dy dz = \iiint \frac{\mathcal{B}}{b_z} dx dy db'' \\ &\approx \int \frac{1}{\langle b_z \rangle} F db'' = \int \frac{1}{\langle b_z \rangle} \int_0^{b''} \mathcal{E}_{\text{net}} db' db'', \quad (35) \end{aligned}$$

where the middle equality is approximate because it has assumed that b_z is uncorrelated with \mathcal{B} on the buoyancy surface, and the last step has used the relationship $F = \int_0^b \mathcal{E}_{\text{net}} db'$ of Eq. (12). The integrand in the last part of Eq. (35) has essentially already been calculated above, since, from Eq. (13), we have $\langle b_z \rangle^{-1} \int_0^b \mathcal{E}_{\text{net}} db' = |\mathcal{E}_{\text{SML}}| d$, and we have plotted $|\mathcal{E}_{\text{SML}}|$ in Fig. 3d. Hence, the volume integral of the magnitude of the diffusive buoyancy flux \mathcal{G} over the abyssal ocean up to a depth of ~ 2000 m is equivalent to the area under the $|\mathcal{E}_{\text{SML}}|$ curve in Fig. 3d from $b = 0$ up to $b = 3.5 \times 10^{-3} \text{ m s}^{-2}$, multiplied by $d = 500$ m. Performing this integral gives \mathcal{G} to be approximately $10^8 \text{ m}^5 \text{ s}^{-3}$, and this scales as $\mathcal{E}_{\text{net}} \Delta b \Delta z$, where we

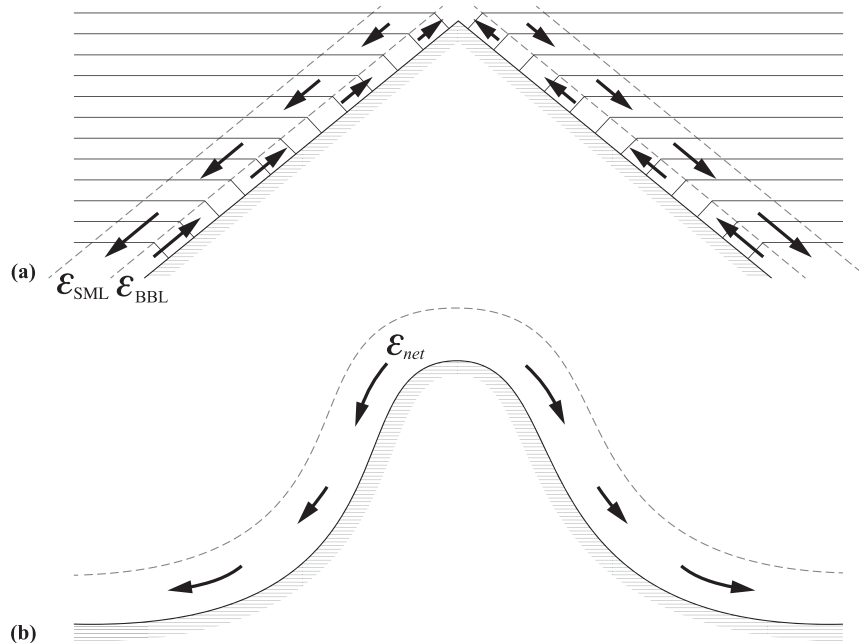


FIG. 6. (a) Sketch of a conical seamount with a constant value of B_0 at the top of the turbulent boundary layer. The upward diapycnal flow in the turbulent boundary layer \mathcal{E}_{BBL} decreases to zero at the top of the seamount, while the downward diapycnal flow in the stratified near-seamount interior \mathcal{E}_{SML} also decreases in magnitude with height. The diapycnal velocities are independent of height in both the BBL and the SML (if b_z is constant). (b) A more realistic (nonconical) seamount cross section is sketched, again with a constant value of B_0 . The dependence of the net diapycnal volume flux $\mathcal{E}_{net} = \mathcal{E}_{BBL} + \mathcal{E}_{SML}$ (which is negative for a conical seamount) on the bottom slope $\tan\theta$ may lead to the smallest values of $|\mathcal{E}_{net}|$ being found at middepth where the bottom slope $\tan\theta$ is largest, with larger magnitudes of \mathcal{E}_{net} both above and below this middepth.

use a typical value of $\mathcal{E}_{net} \approx 13 \text{ Sv} = 13 \times 10^6 \text{ m}^3 \text{ s}^{-1}$, $\Delta b = 3.5 \times 10^{-3} \text{ m s}^{-2}$, and $\Delta z = 2300 \text{ m}$.

To arrive at the volume-integrated dissipation of turbulent kinetic energy, (i) this interior volume-integrated diffusive flux of buoyancy must be converted into volume-integrated dissipation by dividing by the mixing efficiency Γ for which 0.2 is an appropriate value for the stratified interior, obtaining the volume-integrated dissipation of 0.5 TW (after multiplying $\mathcal{G}/0.2$ by 10^3 kg m^{-3}), and (ii) the dissipation in the BBL must be added. With the vertical structure of $\mathcal{B} = \Gamma \varepsilon$ of Fig. 1 in mind, the depth integration of ε above the BBL is then $\mathcal{B}_0 d/0.2$, and if we assume that ε is independent of height within the BBL, then the estimate based on Eq. (35) (which is $\Gamma^{-1} \approx 5$ times this equation) must be multiplied by the ratio $(1 + h/d) \approx 1 + 50/500 = 1.1$. More measurements of ε in the BBL would be needed if this estimate was to be refined.

This conclusion from this analysis of the total amount of dissipation is that it is independent of the height scales h and d , and it is also independent of the bottom slope as given by $\tan\theta$ but rather scales as $\mathcal{E}_{net} \Delta b \Delta z$. So there seems to be no energetic implications of this near-boundary mixing idea. That is, there is no energetic implication of the

realization that there is a lot of interior downwelling and a lot of upwelling in the continental boundary layers. The same energy would be required to upwell a given net volume flux \mathcal{E}_{net} through a buoyancy difference Δb and a height difference Δz no matter whether the upwelling was occurring mainly in the ocean interior (with $\mathcal{B}_z > 0$ and $\mathcal{E}_{SML} > 0$ and perhaps even with vertical sidewalls) or whether there are sloping sidewalls and a large BBL amplification factor $\mathcal{E}_{BBL}/\mathcal{E}_{net}$, as seems to be the case in the real ocean.

The reason for this insensitivity of the gravitational potential energy budget to the large recirculation of diapycnal volume flux, $0.5(\mathcal{E}_{BBL} + |\mathcal{E}_{SML}|)$, is that this large recirculating volume flux enters the gravitational potential energy budget multiplied by the difference between the buoyancy in the BBL and in the SML at constant height, and this buoyancy difference is tiny.

12. Discussion

a. The bottom intensification of mixing versus the one-dimensional view

The simple, one-dimensional, upwelling–diffusion balance in the ocean interior with a constant diapycnal

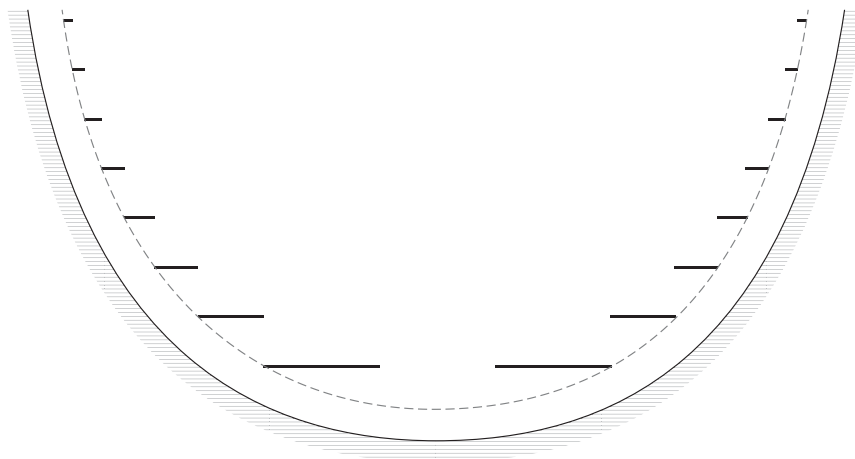


FIG. 7. Sketch of a cross section through an ocean basin whose bottom slope decreases with depth. The length in this plane on which significant diapycnal mixing occurs is proportional to $d/\tan\theta$, and this is shown increasing with depth (d is constant in this figure).

diffusivity implies that the magnitude of the buoyancy flux increases with height, whereas observations of the dissipation of turbulent kinetic energy in the abyssal ocean show the opposite. That is, observations show that the dissipation increases toward the ocean floor, especially where the bottom topography is rough. In this paper, we have included this bottom intensification of the diffusive buoyancy flux, and we have assumed a linear equation of state, thus ignoring the diapycnal downwelling due to thermobaricity and cabbeling.

b. Bottom slope and perimeter: Balancing influences?

A cross section through an ocean basin is sketched in Fig. 7 in which the bottom slope $\tan\theta$ decreases with depth. If the ocean were two-dimensional (i.e., independent of distance into the page of Fig. 7), the area of active diapycnal near-boundary mixing increases proportionally to $d/\tan\theta$, implying that if $\mathcal{B}_0(x, y)$ were a constant value then the area-integrated buoyancy flux F would tend to decrease with height so that $dF/db = \mathcal{E}_{\text{net}}$ would be negative. Countering this tendency in a more realistic three-dimensional situation is the fact that the perimeter (or circumference) around the boundary of the ocean on each buoyancy surface is an increasing function of height (and buoyancy) because ocean basins are better approximated as being circular than being two-dimensional. If in fact the seafloor in Fig. 7 were the lower part of a sphere, then the product of the perimeter and the horizontal distance $d/\tan\theta$ would be constant, independent of the height of the horizontal cut through the sphere. In this situation a constant value of $\mathcal{B}_0(x, y) = \mathcal{B}_0$ would give $dF/db = \mathcal{E}_{\text{net}} = 0$, which is not a valid steady-state solution for the abyss. If on the other

hand, the side boundaries of the three-dimensional ocean have a more or less constant slope, then the geometry more closely approximates the conical ocean of section 7 and net upwelling would occur even if $\mathcal{B}_0(x, y) = \mathcal{B}_0$ is constant. This discussion emphasizes the sensitivity of the net diapycnal volume flux to the details of the area available for active mixing in the SML. It is fascinating that in this SML region the diapycnal volume transport is downward, but the net upward diapycnal transport depends sensitively on the vertical variation of the SML area.

c. The much increased BBL transport with the bottom intensification of mixing

The large diapycnal upwelling transport in the BBL predicted by this study is here contrasted with what would be expected without the bottom intensification of mixing intensity. Consider a conical ocean as in section 7 but now without the bottom intensification of mixing. As before we assume that the stratification b_z is constant along each isopycnal, but it can vary from one isopycnal to another in the vertical. The area-integrated buoyancy flux is $F = \pi R^2 D b_z$, where we will allow the diapycnal diffusivity D to be a function of buoyancy. The diapycnal transport in the BBL is given by Eqs. (2) or (26), namely,

$$\mathcal{E}_{\text{BBL}} = 2\pi R \frac{D}{\tan\theta}, \quad \text{conical ocean, interior mixing,} \quad (37)$$

while the net diapycnal upwelling is given by (using $R_z = 1/\tan\theta$)

$$\mathcal{E}_{\text{net}} = \frac{dF}{db} = 2\pi R \left(\frac{D}{\tan\theta} + 0.5RD_z + 0.5RD \frac{b_{zz}}{b_z} \right). \quad (38)$$

conical ocean, interior mixing

The ratio $\mathcal{E}_{\text{BBL}}/\mathcal{E}_{\text{net}}$ is then

$$\frac{\mathcal{E}_{\text{BBL}}}{\mathcal{E}_{\text{net}}} = \left(1 + 0.5R \tan\theta \frac{D_z}{D} + 0.5R \tan\theta \frac{b_{zz}}{b_z} \right)^{-1}. \quad (39)$$

conical ocean, interior mixing

It is not clear what is an appropriate value to take for R in the abyssal ocean, so we will consider two values. With $R \approx L/(2\pi) \approx (5 \times 10^7 \text{ m})/(2\pi) \approx 10^7 \text{ m}$, $\tan\theta \approx 400^{-1}$, and assuming the inverse vertical length scale $D_z/D + b_{zz}/b_z$ to be dominated by b_{zz}/b_z of about $(1000 \text{ m})^{-1}$, we find that $\mathcal{E}_{\text{BBL}}/\mathcal{E}_{\text{net}} = (1 + 12.5)^{-1}$, implying that only 7.4% of the net diapycnal upwelling occurs in the BBL. Taking $R \approx 10^6 \text{ m}$ gives $\mathcal{E}_{\text{BBL}}/\mathcal{E}_{\text{net}} = (1 + 1.25)^{-1} \approx 0.44$, implying that 44% of the net diapycnal upwelling occurs in the BBL. These values for $\mathcal{E}_{\text{BBL}}/\mathcal{E}_{\text{net}}$ contrast with the value 5 found in the present paper for bottom-intensified diapycnal mixing, that is, we have found that the BBL carries 500% of the net diapycnal upwelling \mathcal{E}_{net} in the abyssal ocean. These very different estimates of the ratio $\mathcal{E}_{\text{BBL}}/\mathcal{E}_{\text{net}}$ are due to the bottom intensification of mixing activity in the present case. By contrast, when the diapycnal mixing is assumed to occur uniformly along density surfaces, the whole area of the isopycnal contributes to the diapycnal diffusive buoyancy flux.

d. The case where F is depth independent

The special case when the magnitude of the area-integrated diffusive buoyancy flux F is independent of buoyancy is here shown to be incompatible with a global steady state. In this case, we have $dF/db = \mathcal{E}_{\text{BBL}} + \mathcal{E}_{\text{SML}} = \mathcal{E}_{\text{net}} = 0$ [from Eq. (3)], so that the local downwelling in the stratified interior SML is equal to the local upwelling in the BBL. This is a perfectly acceptable balance for a localized region of mixing, but for a globally integrated situation, having no net diapycnal upwelling ($\mathcal{E}_{\text{net}} = 0$) is incompatible with a steady-state solution in which there is vertical stratification in the abyss since a strictly positive mean diapycnal volume flux $\mathcal{E}_{\text{net}} > 0$ is needed to balance the diffusive buoyancy flux F that enters the volume that is bounded above by the b buoyancy surface [see Eq. (B1) of appendix B where the volume-integrated buoyancy budget requires that \mathcal{E}_{net} be positive since F is positive].

e. Implications for the Stommel–Arons abyssal circulation

What are the implications of our results for the Stommel–Arons circulation? Some of the implications of ocean hypsometry have already been pointed out by McDougall [1989, see his Eqs. (15)–(16) and Fig. 6 therein] and by Rhines (1993, p. 137–140 and Figs. 19 and 20 therein). These authors pointed out that if the diapycnal upwelling is assumed to be uniformly distributed over isopycnals, then both (i) the increasing area of isopycnals with height and (ii) entrainment into the sinking plume of AABW induce vortex stretching in the ocean interior of the opposite sign of Stommel–Arons. In the present work, we have explored the implications of the bottom-intensified nature of diapycnal mixing, and we have shown that the effects of this bottom intensification on the structure of the diapycnal velocity varies both laterally and vertically, resulting in a complex pattern of stretching and squeezing of water columns.

Imagine an ocean basin that is roughly circular with most of the inner area exhibiting neither diapycnal upwelling nor downwelling but with an annulus of width of 4° , exhibiting strong diapycnal downwelling of $\sim 80 \text{ Sv}$ and an even thinner (0.2°) outer annulus right against the continent in which there is strong upwelling of $\sim 100 \text{ Sv}$. This is illustrated in Fig. 4. Within the region of diapycnal downwelling, the downward diapycnal velocity increases in magnitude with depth, implying vertical vortex stretching of the same sign as Stommel–Arons (i.e., $e_z > 0$). The full implications of this vortex stretching clearly needs further research. Rhines' (1993, p. 142) very nice review ended with the phrase “pointed study of ‘in-cropping’ is called for.” The present paper, de Lavergne et al. (2016), and Ferrari et al. (2016) may be regarded as some small steps in that direction.

f. Sensitivity of ocean models to d

In a numerical study, Oka and Niwa (2013) found that the deep Pacific circulation was sensitive to the choice of the vertical scale height d over which the near-boundary diapycnal mixing varied. The sensitivity can be explained as being due to the area of significant diapycnal mixing on each isopycnal being proportional to d through the horizontal length scale $d/\tan\theta$ (see Figs. 2b and 7). This implies that the area-integrated diffusive buoyancy flux F (and hence $\int_0^b \mathcal{E}_{\text{net}} db'$) varies proportionally with d . The same proportionality with d applies to the magnitude of the volume-integrated buoyancy flux. If the volume-integrated buoyancy flux were kept constant as d was changed in a forward numerical ocean model by making $\mathcal{B}_0(x, y)$ (or perhaps the diapycnal eddy diffusivity)

at the top of the turbulent boundary layer be proportional to d^{-1} , we expect that the net overturning circulation would be rather insensitive to the vertical e -folding length scale d .

13. Conclusions

A Walin-like buoyancy budget has been performed on volumes bounded by buoyancy surfaces that intersect the seafloor. We have incorporated the observed increase of diapycnal mixing intensity in the stratified interior toward the seafloor; this downward increase in mixing drives downward diapycnal advection in the stratified fluid. We also prescribed that the buoyancy flux becomes zero (or to match the geothermal heat flux) at the bottom of a turbulent bottom boundary layer (BBL) right above the seafloor; this downward decrease in the magnitude of the buoyancy flux in the BBL drives an upward diapycnal advection along sloping bottom boundary layers. We find the following:

- The upward diapycnal volume transport in the turbulent BBL is typically several times as large as the net upwelling of AABW in the abyss.
- This implies that there is substantial cancellation between the large upwelling in the BBL and the (almost as large) downwelling in the stratified mixing layer (SML) that lies in the stratified ocean but is near the seafloor where the diapycnal mixing is significant.
- The buoyancy budget for the whole volume below a certain buoyancy surface is given by Eq. (12), which shows that the magnitude of the area-integrated diffusive buoyancy flux across this buoyancy surface is equal to the integral with respect to the buoyancy of the net diapycnal upwelling throughout the ocean below this buoyancy surface.
- The main findings of this paper are the simple relations (13) and (14) that have been used to estimate that the volume flux upwelling in the turbulent BBLs globally is as much as 5 times the net diapycnal upwelling of bottom waters in the abyss and that the near-boundary diapycnal sinking in the SML is as much as 4 times this net upwelling. The amplification factor $\mathcal{E}_{\text{BBL}}/\mathcal{E}_{\text{net}}$ was found to be between 2 and 3 in Ferrari et al. (2016), and it depends on the way that the net diapycnal upwelling \mathcal{E}_{net} varies with height (or buoyancy) in the abyss [as can be seen in Eq. (14)].
- Our approach has been based on the buoyancy equation, so that the large epineutral advection and diffusion processes do not enter or complicate our method. While these strong epineutral processes are invisible to our approach, they will be effective in

spreading any tracer signature of the near-boundary mixing processes into the ocean interior.

- The circulation we find is driven by the diffusive flux of buoyancy in the stratified interior ocean, with the magnitude of the buoyancy flux being strongest near the BBL. This is very different to previous boundary mixing theories where the mixing was assumed to originate at the boundary itself and was often mostly very near the boundary in water that is very weakly stratified.
- We have shown that in order to upwell 100 Sv across isopycnals in the BBL, the turbulent diffusivity immediately above the BBL must be approximately $D_0 \approx 5 \times 10^{-3} \text{ m}^2 \text{ s}^{-1}$ on average along the in-crop line of a buoyancy surface. Clearly, this is a large diapycnal diffusivity, and it remains to be seen if this will prove to be a realistic estimate.

Acknowledgments. This work was done while TJMcD was visiting the Woods Hole Oceanographic Institution and the Massachusetts Institute of Technology where the generosity of the Houghton fellowship is gratefully acknowledged. Paul Barker is thanked for doing the calculations underlying Fig. 3, and Louise Bell of Louise Bell Graphic Design (Tasmania) is thanked for preparing the other illustrations. We gratefully acknowledge Australian Research Council support through Grant FL150100090 (T. McD) and National Science Foundation support through Grant OCE-1233832 (R. F.)

APPENDIX A

Diapycnal Volume Fluxes Caused by Interior Diffusive Buoyancy Fluxes and by Geothermal Heating

Here, we analyze the volume and buoyancy budgets for (i) the turbulent BBL region contained between a pair of buoyancy surfaces in Fig. 2a and (ii) for the full shaded volume in Fig. 2b, which contains both the BBL and the SML in which the diapycnal mixing is significantly nonzero. The upper buoyancy surface attracts the label u while l stands for the lower buoyancy surface. These volume-integrated buoyancy budgets are an application of the Walin (1982) methodology, applied to the geometry of the bottom boundary and near-boundary regions; the Walin methodology is more commonly applied to the outcropping of isopycnals at the sea surface.

The epineutral advection of water into the shaded region of Fig. 2a from the interior ocean is labeled

Q_{epiBBL} and the conservation of volume for this region is (without assuming it is in steady state)

$$(V_{\text{BBL}})_t = \mathcal{E}'_{\text{BBL}} - \mathcal{E}''_{\text{BBL}} + Q_{\text{epiBBL}}, \quad (\text{A1})$$

while the buoyancy budget is

$$\begin{aligned} & \frac{1}{2}(b^l + b^u)(V_{\text{BBL}})_t \\ &= \mathcal{E}'_{\text{BBL}} b^l - \mathcal{E}''_{\text{BBL}} b^u + \frac{1}{2}(b^l + b^u)Q_{\text{epiBBL}} + F^{\text{geo}} + \mathcal{D}, \end{aligned} \quad (\text{A2})$$

where \mathcal{D} is the diffusive buoyancy flux entering at the top of the BBL, being the area integral of the corresponding nonadvective buoyancy flux per unit horizontal area between points a and b (and into the page) at the top of the BBL, $\mathcal{B}_0(x, y) \cos\theta$. The buoyancy flux entering the BBL across the seafloor F^{geo} is $g\alpha$ times the corresponding flux of Conservative Temperature, so that F^{geo} is [from appendix A.21 of IOC et al. (2010)] the geothermal heat flux (in watts) times $g\alpha/(\rho\hat{h}_\theta)$, where g is the gravitational acceleration, α is the thermal expansion coefficient with respect to Conservative Temperature, ρ is in situ density, and \hat{h}_θ is the partial derivative of specific enthalpy with respect to Conservative Temperature at constant Absolute Salinity and pressure [see appendix A.21 of IOC et al. (2010)]. This partial derivative is given by (from McDougall 2003) $\hat{h}_\theta = c_p^0(T_0 + t)/(T_0 + \theta)$ (where $T_0 = 273.15\text{ K}$, θ is the potential temperature, and t is the in situ temperature, both on the Celsius temperature scale), which varies very little from the constant value $c_p^0 \equiv 3991.86795711963\text{ J kg}^{-1}\text{ K}^{-1}$ defined by the International Thermodynamic Equation Of Seawater—2010 (TEOS-10). Even at a depth of 4000 m \hat{h}_θ is different from c_p^0 by only 0.15%; by comparison, the uncertainty in the thermal expansion coefficient is $\pm 1\%$ [the rms uncertainty in the thermal expansion coefficient is $0.73 \times 10^{-6}\text{ K}^{-1}$; see appendix K of IOC et al. (2010)]. Hence, we take $g\alpha/(\rho\hat{h}_\theta)$ to be $g\alpha/(\rho c_p^0)$. If the geothermal heat flux per unit of exactly horizontal area is $J\text{ W m}^{-2}$, then the geothermal buoyancy flux per unit area of sloping seafloor is $G \cos\theta$, where G is defined to be the flux of buoyancy into the ocean per unit of exactly horizontal area due to the geothermal heat flux: $G = g\alpha J/(\rho c_p^0)$.

Subtracting $(1/2)(b^u + b^l)$ times Eq. (A1) from Eq. (A2) and taking the limit as $(b^u - b^l) = \Delta b \rightarrow 0$ so that $(1/2)(\mathcal{E}'_{\text{BBL}} + \mathcal{E}''_{\text{BBL}}) \rightarrow \mathcal{E}_{\text{BBL}}$, we find

$$\mathcal{E}_{\text{BBL}} \Delta b = F^{\text{geo}} + \mathcal{D}. \quad (\text{A3})$$

Neither the unsteadiness of the situation nor the existence of the epineutral volume flux Q_{epiBBL} affects this simple balance between the sum of the area-integrated geothermal heat flux F^{geo} and the diffusive (i.e., the nonadvective) area-integrated buoyancy flux \mathcal{D} being balanced by the advective volume flux \mathcal{E}_{BBL} of the fluid in the BBL toward less dense water. These geothermal and diffusive buoyancy fluxes F^{geo} and \mathcal{D} are both fluxes of buoyancy into the BBL, and they can be expressed as the area integral of the corresponding fluxes per unit of the sloping area between points a and b at the top of the turbulent boundary layer $G \cos\theta$ and $\mathcal{B}_0 \cos\theta$. The element of area integration, per unit distance into the page of Fig. 2, is $\Delta b/(b_z \sin\theta)$, so that the geothermal buoyancy flux and the diffusive buoyancy flux \mathcal{D} are

$$F^{\text{geo}} = \Delta b \int \frac{G}{b_z} \frac{1}{\tan\theta} dc \quad \text{and} \quad \mathcal{D} = \Delta b \int \frac{\mathcal{B}_0}{b_z} \frac{1}{\tan\theta} dc, \quad (\text{A4})$$

where c is the distance measured into the page of Fig. 2 along the boundary at the top of the turbulent boundary layer. Substituting F^{geo} and \mathcal{D} from Eq. (A4) into Eq. (A3) gives

$$\mathcal{E}_{\text{BBL}} = \int \frac{G + \mathcal{B}_0}{b_z} \frac{1}{\tan\theta} dc. \quad (\text{A5})$$

Note that this expression for the upward volume flux in the BBL (\mathcal{E}_{BBL}) is independent of the vertical distance d over which the dissipation decreases in the vertical. This result of the buoyancy and volume budgets is an application of the Walin (1982) approach to this control volume, where we have ignored any diapycnal diffusion of buoyancy along the direction of the boundary in the BBL because the gradient of buoyancy in this direction is so small at $b_z \sin\theta$ and the lateral distance over which this buoyancy flux varies is so much larger than the thickness of the boundary layer.

In the above derivation we have taken the element of area integration, per unit distance into the page of Fig. 2, to be $\Delta b/(b_z \sin\theta)$, and this is a linearization that clearly fails when $\sin\theta$ approaches zero. A more accurate derivation of Eq. (A5) would stay closer to the Walin (1982) approach (see, e.g., Marshall et al. 1999), giving

$$\mathcal{E}_{\text{BBL}} = \frac{d}{db} \iint_{A_{\text{in}}(b^l < b)} (G + \mathcal{B}_0) dA, \quad (\text{A6})$$

where the area integral is taken over all the ocean floor (in-crop area) in this region that has buoyancy less than b . Again, G and \mathcal{B}_0 are the buoyancy fluxes per unit of exactly horizontal area, and $dA = dx dy$ is the element of exactly horizontal area. This convention is not

fundamental or important; it is done simply because ocean models have latitude and longitude as coordinates. We will use the linearized formulation, Eq. (A5), in this paper, but it should be understood that this is just a convenient way of writing the exact expression, Eq. (A6), for \mathcal{E}_{BBL} .

Note that \mathcal{B}_0/b_z in Eq. (A5) is the value of the diapycnal diffusivity in the stratified fluid just above the BBL, D_0 , and Eq. (A5) implies that the diapycnal transport in the BBL due to diapycnal diffusion, per unit length into the page, is proportional to this diapycnal diffusivity D_0 and inversely proportional to the slope $\tan\theta$ of the seafloor. This is reminiscent of Thorpe (1987) and Garrett's (1990) results for their diapycnal transport streamfunction $\Psi = D_\infty/(\tan\theta)$ due to near-boundary mixing, although their result was based on a two-dimensional ocean geometry that was uniform into the page, with their buoyancy frequency being independent of height and with the diapycnal diffusivity being a function only of distance from the sloping boundary; D_∞ was the diapycnal diffusivity far from the boundary. We have made none of these assumptions and, by contrast, our result Eq. (A5) applies only to the part of the diapycnal transport that occurs in the BBL.

We now write budget statements for volume and buoyancy for the volume of shaded fluid between the two isopycnals in Fig. 2b. This control volume includes both the fluid in the turbulent BBL and the fluid in the ocean interior in which there is significant nonzero dissipation (the SML). In practice, we can think of this region as extending to a horizontal distance where the buoyancy surface is say $2d$ above the top of the BBL. At that location the magnitude of the vertical flux of buoyancy is quite small at $\mathcal{B}_0 \exp(-2) \approx 0.135\mathcal{B}_0$, assuming an exponential function of height with vertical scale height d . The volume V of the control volume is allowed to change with time, and it receives the volume flux Q_{epi} at the average buoyancy $(1/2)(b^l + b^u)$ by epineutral advection from the adiabatic interior ocean. The volume budget is

$$V_t = \mathcal{E}_{\text{BBL}}^l - \mathcal{E}_{\text{BBL}}^u + \mathcal{E}_{\text{SML}}^l - \mathcal{E}_{\text{SML}}^u + Q_{\text{epi}}, \quad (\text{A7})$$

while its buoyancy budget is

$$\begin{aligned} \frac{1}{2}(b^l + b^u)V_t &= \mathcal{E}_{\text{BBL}}^l b^l - \mathcal{E}_{\text{BBL}}^u b^u + \mathcal{E}_{\text{SML}}^l b^l - \mathcal{E}_{\text{SML}}^u b^u \\ &+ F^u - F^l + F^{\text{geo}} + \frac{1}{2}(b^l + b^u)Q_{\text{epi}}, \end{aligned} \quad (\text{A8})$$

where the volume-averaged buoyancy of the shaded fluid $(1/2)(b^l + b^u)$ does not vary with time as we are following these same two buoyancy surfaces through time. Technically, we should include a diffusive flux of buoyancy across the area between points c and d , but we

assume that the diffusive buoyancy flux here has diminished to a near-zero value, which we ignore. From the buoyancy budget [Eq. (A8)] is now subtracted $(1/2)(b^l + b^u)$ times the volume conservation equation [Eq. (A7)], obtaining

$$\begin{aligned} (b^u - b^l) \left[\frac{1}{2}(\mathcal{E}_{\text{BBL}}^l + \mathcal{E}_{\text{BBL}}^u) \right. \\ \left. + \frac{1}{2}(\mathcal{E}_{\text{SML}}^u + \mathcal{E}_{\text{SML}}^l) \right] &= F^u - F^l + F^{\text{geo}}. \end{aligned} \quad (\text{A9})$$

Taking the limit as the buoyancy difference between the surfaces tends to zero, we have

$$\mathcal{E}_{\text{net}} \equiv \mathcal{E}_{\text{BBL}} + \mathcal{E}_{\text{SML}} = \frac{dF}{db} + \int \frac{G}{b_z} \frac{1}{\tan\theta} dc, \quad (\text{A10})$$

where dF/db is the rate at which the isopycnally area-integrated magnitude of the turbulent diffusive buoyancy flux F [see Eq. (1)] varies with respect to the buoyancy label b of the isopycnals, while the corresponding quantity for the geothermal buoyancy flux, namely, $F^{\text{geo}}/\Delta b$ in the limit $\Delta b \rightarrow 0$, has been written using Eq. (A4).

The key results of this appendix, Eqs. (A5) and (A10), are the Walin buoyancy budget approach applied to this geometry [see also Garrett et al. (1995) and Marshall et al. (1999) for clear expositions of the Walin approach to volume-integrated buoyancy budgets]. The new feature is that we have separated the budgets into the region of the BBL, where the diapycnal transport is always positive $\mathcal{E}_{\text{BBL}} > 0$ (both because of the geothermal heat flux and the interior mixing processes), and the near-boundary SML of the interior, where we will see that the diapycnal transport is always negative $\mathcal{E}_{\text{SML}} < 0$. The simplifications that we have been able to make are (i) that the diffusive flux of buoyancy along the boundary in the BBL is tiny (and its divergence is even smaller by a factor of order $0.5h \sin^2\theta b_{zz}/b_z$ compared with the \mathcal{B}_0 term) so this flux has been ignored; and (ii) because the interior mixing intensity is taken to decay in the vertical, it also decays along a buoyancy surface sufficiently far from the boundary, and this has enabled us to ignore any diffusion of buoyancy on the right-hand side of the shaded fluid in Fig. 2b. In this paper, we have not concentrated on the physical processes that cause the vertical profile of the turbulent buoyancy flux, so that, for example, the intriguing and asymmetric physics of the arrested Ekman layer effect (Garrett et al. 1993) could be regarded as being part of our formulation only if its turbulent buoyancy fluxes were regarded as having been included as a contributor to our assumed exponential decay of the magnitude of the buoyancy flux with height above the BBL.

While the sketch shown in Fig. 2 shows the isopycnals to be normal to the boundary throughout the BBL, this is not a requirement of these buoyancy budgets. The surfaces of constant buoyancy can be drawn as smooth curves, and the results of this appendix continue to apply. The buoyancy budgets in this paper rely on separating the BBL and SML regions. These regions are separated by the line along which the diapycnal velocity is zero, with the diapycnal velocity being positive in the BBL and negative in the SML. That is, the BBL and SML regions are separated by the height of the maximum magnitude of the buoyancy flux per unity area as a function of height on Fig. 1. Clearly at this height the vertical stability b_z must be nonzero, for otherwise the mixing efficiency and the magnitude of the buoyancy flux would be zero rather than being a maximum.

Equations (A5) and (A10) provide expressions for the diapycnal volume transports in (i) the BBL, \mathcal{E}_{BBL} , and (ii) across the entire isopycnal in this region \mathcal{E}_{net} . The difference between these two equations provides an expression for the diapycnal transport across the SML of the same isopycnal, namely,

$$\mathcal{E}_{\text{SML}} = \frac{dF}{db} - \int \frac{\mathcal{B}_0}{b_z} \frac{1}{\tan\theta} dc. \quad (\text{A11})$$

This same equation can be found by performing the above Walin-type buoyancy budget for the shaded fluid in the SML of Fig. 2b, that is, for the shaded region of that figure but excluding the part in the BBL. This SML region of Fig. 2 has the diffusive buoyancy flux \mathcal{D} exiting across the boundary a - b so that the SML loses buoyancy diffusively at the rate $\mathcal{D} + F^l - F^u$, and even in the simple case where F^u and F^l are equal, the interior SML fluid suffers a diffusive loss of buoyancy. This net diffusive loss of buoyancy $\mathcal{D} + F^l - F^u$ may seem counterintuitive in a steady-state situation, but it is balanced by the advective gain of buoyancy since the diapycnal volume transport \mathcal{E}_{SML} is negative (i.e., downward flow through isopycnals).

Equation (A11) states that knowledge of both dF/db and the diffusive buoyancy flux just above the BBL \mathcal{B}_0 is sufficient to give the diapycnal volume flux in the SML \mathcal{E}_{SML} . In the text, we have a different expression for \mathcal{E}_{SML} [Eq. (7)], which is written as the integral of \mathcal{B}_z/b_z over the area of a buoyancy surface in the SML. Are Eqs. (7) and (A11) consistent? Combining these equations while using Eq. (A6) and the definition of F of Eq. (1), we find

$$\iint \frac{\mathcal{B}_z(b, x, y)}{b_z} dx dy = \frac{d}{db} \iint \mathcal{B}(b, x, y) dx dy - \frac{d}{db} \iint_{A_{\text{in}}(b' < b)} \mathcal{B}_0 dx dy. \quad (\text{A12})$$

Here, we will show that this equation is a mathematical truism [i.e., it is obeyed by any $\mathcal{B}(b, x, y)$ field] with no predictive value per se, so that we conclude that Eqs. (7) and (A11) are consistent with each other. Writing the negative of the buoyancy flux $\mathcal{B}(b, x, y)$ more generally as the three-dimensional vector \mathcal{B} , the left-hand side of Eq. (A12) is the area integral on a buoyancy surface in the SML of $\nabla \cdot \mathcal{B}/|\nabla b|$, and using Gauss' divergence theorem the right-hand side can be written in terms of a volume integral of $\nabla \cdot \mathcal{B}$ in the SML region, so that Eq. (A12) is equivalent to the standard mathematical result (see Marshall et al. 1999):

$$\iint_{A(b)} \frac{a(\mathbf{x}, t)}{|\nabla b|} dA = \frac{d}{db} \iiint_{V(b' < b)} a(\mathbf{x}, t) dV, \quad (\text{A13})$$

where in our case $a(\mathbf{x}, t) = \nabla \cdot \mathcal{B}$, $A(b)$ is the area of the b buoyancy surface in the SML, and $V(b' < b)$ is the volume of seawater in the SML region that lies below the b buoyancy surface, that is, it is the volume that lies below the b buoyancy surface but excludes the BBL.

APPENDIX B

Steady-State Volume-Integrated Buoyancy Budget

Consider the steady-state situation in which a plume of very dense AABW sinks through the stratified ocean as shown in Fig. B1. The control volume we consider in this appendix is below the buoyancy surface b in the BBL, SML, and ocean interior and is then extended horizontally to the ocean boundary through the sinking AABW plume. In the body of this paper and in appendix A, the sinking AABW plume region has not been separately considered.

The volume flux rising through the nonplume part of the b surface is \mathcal{E}_{net} , and in a steady state this is equal to the volume flux of the sinking very dense AABW plume that punches through a small part of the upper surface of the control volume. The buoyancy budget for the whole control volume represents the balance between the diffusive flux of buoyancy F that enters the top of the control volume being balanced by the advection of buoyancy out of the control volume due to the volume flux \mathcal{E}_{net} entering at one (small) value of buoyancy b_{BWP} and leaving at another, namely, at b . That is, the volume-integrated buoyancy budget is

$$F = \mathcal{E}_{\text{net}}(b)[b - b_{\text{BWP}}(b)], \quad (\text{B1})$$

where both the volume flux of the AABW plume \mathcal{E}_{net} and its average buoyancy b_{BWP} can be regarded as being functions of the interior buoyancy b at the same height.

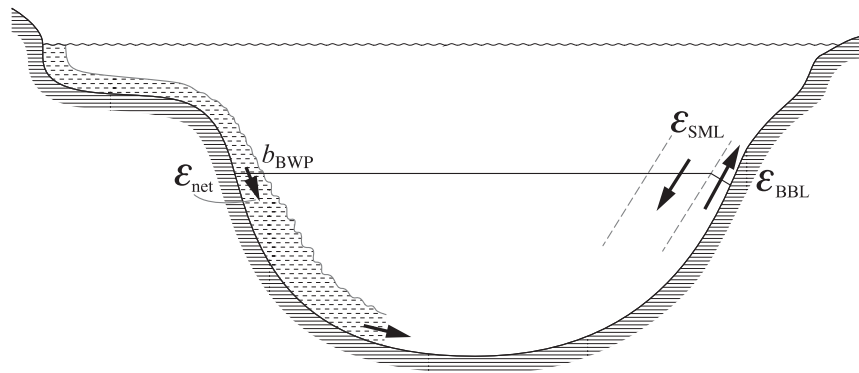


FIG. B1. An ocean cross section through the sinking very dense bottom water plume whose buoyancy is b_{BWP} . With the ocean in a steady state, the volume transport of the bottom water plume is equal to the net diapycnal upwelling throughout the rest of the ocean: $\mathcal{E}_{\text{net}} = \mathcal{E}_{\text{BBL}} + \mathcal{E}_{\text{SML}}$. In the buoyancy budget analysis of appendix A we have considered the diffusive and advective fluxes of buoyancy across the buoyancy surface in the BBL and throughout the stratified ocean interior but excluding the region inside the sinking bottom water plume. The volume-integrated buoyancy budget of Eq. (B1) applies to the volume beneath the same buoyancy surface in the BBL and the stratified ocean interior, and in this case the surface is completed by extending it horizontally through the sinking bottom water plume as shown in the figure.

This is a different expression to Eq. (12) in the text, namely, $F = \int_{b_{\text{min}}}^b \mathcal{E}_{\text{net}} db'$, and in order to prove that they are consistent, we need to prove that the buoyancy derivative of Eq. (B1) is \mathcal{E}_{net} .

From plume theory in a stratified fluid [e.g., Eqs. (2)–(3) of Morton et al. (1956)] the buoyancy budget of the entraining dense AABW plume can be cast in terms of the derivatives with respect to buoyancy as

$$\frac{d}{db} [\mathcal{E}_{\text{net}}(b)b_{\text{BWP}}(b)] = b \frac{d}{db} [\mathcal{E}_{\text{net}}(b)], \quad (\text{B2})$$

and this applies whether the AABW plume is entraining or detraining (Baines 2005). Differentiating Eq. (B1) with respect to b and using Eq. (B2) shows that $dF/db = \mathcal{E}_{\text{net}}$, and hence the volume-integrated buoyancy budget [Eq. (B1)] is consistent with Eq. (12), namely, $F = \int_{b_{\text{min}}}^b \mathcal{E}_{\text{net}} db'$.

REFERENCES

- Armi, L., 1979: Reply to comment by C. Garrett. *J. Geophys. Res.*, **84**, 5097–5098, doi:10.1029/JC084iC08p05097.
- Baines, P. G., 2005: Mixing regimes for the flow of dense fluid down slopes into stratified environments. *J. Fluid Mech.*, **538**, 245–267, doi:10.1017/S0022112005005434.
- de Lavergne, C., G. Madec, J. Le Sommer, G. A. J. Nurser, and A. C. Naveira Garabato, 2016: On the consumption of Antarctic Bottom Water in the abyssal ocean. *J. Phys. Oceanogr.*, **46**, 635–661, doi:10.1175/JPO-D-14-0201.1.
- Emile-Geay, J., and G. Madec, 2009: Geothermal heating, diapycnal mixing and the abyssal circulation. *Ocean Sci.*, **5**, 203–217, doi:10.5194/os-5-203-2009.
- Ferrari, R., A. Mashayek, T. J. McDougall, M. Nikurashin, and J.-M. Campin, 2016: Turning ocean mixing upside down. *J. Phys. Oceanogr.*, **46**, 2239–2261, doi:10.1175/JPO-D-15-0244.1.
- Garrett, C., 1990: The role of secondary circulation in boundary mixing. *J. Geophys. Res.*, **95**, 3181–3188, doi:10.1029/JC095iC03p03181.
- , 1991: Marginal mixing theories. *Atmos.–Ocean*, **29**, 313–319, doi:10.1080/07055900.1991.9649407.
- , 2001: An isopycnal view of near-boundary mixing and associated flows. *J. Phys. Oceanogr.*, **31**, 138–142, doi:10.1175/1520-0485(2001)031<0138:AIVONB>2.0.CO;2.
- , P. MacCready, and P. Rhines, 1993: Boundary mixing and arrested Ekman layers: Rotating stratified flow near a boundary. *Annu. Rev. Fluid Mech.*, **25**, 291–323, doi:10.1146/annurev.fl.25.010193.001451.
- , K. Speer, and E. Tragou, 1995: The relationship between water mass formation and the surface buoyancy flux, with application to Phillips' Red Sea model. *J. Phys. Oceanogr.*, **25**, 1696–1705, doi:10.1175/1520-0485(1995)025<1696:TRBWMF>2.0.CO;2.
- Gouretski, V. V., and K. P. Koltermann, 2004: WOCE global hydrographic climatology: A technical report. Berichte des Bundesamtes für Seeschifffahrt und Hydrographie 35/2004, 52 pp.
- IOC, SCOR, and IAPSO, 2010: The International Thermodynamic Equation of Seawater—2010: Calculation and use of thermodynamic properties. Intergovernmental Oceanographic Commission, Manuals and Guides 56, 220 pp. [Available online at <http://www.teos-10.org/pubs/TEOS-10-Manual.pdf>.]
- Jackett, D. R., and T. J. McDougall, 1997: A neutral density variable for the world's oceans. *J. Phys. Oceanogr.*, **27**, 237–263, doi:10.1175/1520-0485(1997)027<0237:ANDVFT>2.0.CO;2.
- Klocker, A., and T. J. McDougall, 2010: Influence of the nonlinear equation of state on global estimates of diapycnal advection and diffusion. *J. Phys. Oceanogr.*, **40**, 1690–1709, doi:10.1175/2010JPO4303.1.

- Kunze, E., E. Firing, J. M. Hamilton, and T. K. Chereskin, 2006: Global abyssal mixing inferred from lowered ADCP shear and CTD strain profiles. *J. Phys. Oceanogr.*, **36**, 1553–1576, doi:10.1175/JPO2926.1.
- Lumpkin, R., and K. Speer, 2007: Global ocean meridional overturning. *J. Phys. Oceanogr.*, **37**, 2550–2562, doi:10.1175/JPO3130.1.
- Marshall, J. C., D. Jamous, and J. Nilsson, 1999: Reconciling thermodynamic and dynamic methods of computation of water-mass transformation rates. *Deep-Sea Res. I*, **46**, 545–572, doi:10.1016/S0967-0637(98)00082-X.
- McDougall, T. J., 1984: The relative roles of diapycnal and isopycnal mixing on subsurface water mass conversion. *J. Phys. Oceanogr.*, **14**, 1577–1589, doi:10.1175/1520-0485(1984)014<1577:TRRODA>2.0.CO;2.
- , 1989: Dianeutral advection. *Parameterization of Small-Scale Processes: Proc. 'Aha Huliko'a Hawaiian Winter Workshop*, Honolulu, HI, University of Hawai'i at Mānoa, 289–315.
- , 2003: Potential enthalpy: A conservative oceanic variable for evaluating heat content and heat fluxes. *J. Phys. Oceanogr.*, **33**, 945–963, doi:10.1175/1520-0485(2003)033<0945:PEACOV>2.0.CO;2.
- Morton, B. R., G. Taylor, and J. S. Turner, 1956: Turbulent gravitational convection from maintained and instantaneous sources. *Proc. Roy. Soc. London*, **A234**, 1–23, doi:10.1098/rspa.1956.0011.
- Munk, W. H., 1966: Abyssal recipes. *Deep-Sea Res. Oceanogr. Abstr.*, **13**, 707–730, doi:10.1016/0011-7471(66)90602-4.
- , and C. Wunsch, 1998: Abyssal recipes II: Energetics of tidal and wind mixing. *Deep-Sea Res. I*, **45**, 1977–2010, doi:10.1016/S0967-0637(98)00070-3.
- Nikurashin, M., and R. Ferrari, 2013: Overturning circulation driven by breaking internal waves in the deep ocean. *Geophys. Res. Lett.*, **40**, 3133–3137, doi:10.1002/grl.50542.
- Oka, A., and Y. Niwa, 2013: Pacific deep circulation and ventilation controlled by tidal mixing away from the sea bottom. *Nat. Commun.*, **4**, 2419, doi:10.1038/ncomms3419.
- Osborn, T. R., 1980: Estimates of the local rate of vertical diffusion from dissipation measurements. *J. Phys. Oceanogr.*, **10**, 83–89, doi:10.1175/1520-0485(1980)010<0083:EOTLRO>2.0.CO;2.
- Phillips, O. M., 1970: On flows induced by diffusion in a stably stratified fluid. *Deep-Sea Res. Oceanogr. Abstr.*, **17**, 435–443, doi:10.1016/0011-7471(70)90058-6.
- , J.-H. Shyu, and H. Salmun, 1986: An experiment on boundary mixing: Mean circulation and transport rates. *J. Fluid Mech.*, **173**, 473–499, doi:10.1017/S0022112086001234.
- Polzin, K. L., J. M. Toole, J. R. Ledwell, and R. W. Schmitt, 1997: Spatial variability of turbulent mixing in the abyssal ocean. *Science*, **276**, 93–96, doi:10.1126/science.276.5309.93.
- Rhines, P. B., 1993: Oceanic general circulation: Wave and advection dynamics. *Modelling Oceanic Climate Interactions*, J. Willebrand and D. L. T. Anderson, Eds., Springer-Verlag, 67–149.
- St. Laurent, L., J. M. Toole, and R. W. Schmitt, 2001: Buoyancy forcing by turbulence above rough topography in the abyssal Brazil Basin. *J. Phys. Oceanogr.*, **31**, 3476–3495, doi:10.1175/1520-0485(2001)031<3476:BFBTAR>2.0.CO;2.
- Talley, L. D., 2013: Closure of the global overturning circulation through the Indian, Pacific, and Southern Oceans. *Oceanography*, **26**, 80–97, doi:10.5670/oceanog.2013.07.
- Thorpe, S. A., 1987: Current and temperature variability on the continental slope. *Philos. Trans. Roy. Soc. London*, **A323**, 471–517, doi:10.1098/rsta.1987.0100.
- Walín, G., 1982: On the relation between sea-surface heat flow and thermal circulation in the ocean. *Tellus*, **34**, 187–195, doi:10.1111/j.2153-3490.1982.tb01806.x.
- Waterhouse, A. F., and Coauthors, 2014: Global patterns of diapycnal mixing from measurements of the turbulent dissipation rate. *J. Phys. Oceanogr.*, **44**, 1854–1872, doi:10.1175/JPO-D-13-0104.1.
- Wunsch, C., 1970: On oceanic boundary mixing. *Deep-Sea Res. Oceanogr. Abstr.*, **17**, 293–301, doi:10.1016/0011-7471(70)90022-7.